Design and fabrication of a solar simulator

A final year project report

Presented to

SCHOOL OF MECHANICAL AND MANUFACTURING ENGINEERING
Department of Mechanical Engineering
NUST
ISLAMABAD, PAKISTAN

In Partial Fulfillment
of the Requirements for the Degree of
Bachelors of Mechanical Engineering

by

Hamza Butt
Muaaz Farooq
Muhammad Abdullah Haroon Shah

June 2017

EXAMINATION COMMITTEE

We hereby recommend that the dissertation prepared under our supervision by:

Hamza Butt -*NUST201306144BSMME11113F*

Muaaz Farooq- *NUST201305701BSMME11113F*

Muhammad Abdullah Haroon Shah -*NUST201306224BSMME11113F*

Titled: "**Design and fabrication of a solar simulator**" be accepted in partial fulfillment of the requirements for the award of **BE Mechanical Engineering degree**.

Supervisor: **Dr. Muhammad Sajid** **Assistant Professor**	Dated:
Committee Member: **Dr. Emad Uddin** **Assistant Professor**	Dated:
Committee Member: **Mr. Hafiz Muhammad Abd Ur Rehman**	Dated:

_____ _____

(Head of Department) (Date)

COUNTERSIGNED

Dated: _____ _____

(Dean / Principal)

ABSTRACT

Solar simulator for evaluating efficiency and power output of photo voltaic (PV) cells with rise in temperature, has been designed and fabricated. Solar simulator is capable enough to provide the necessary and required conditions for testing of single mono crystalline silicon (40mm x 40 mm) PV cell. Light source, concentrator, flux measurement system, light spectrometer and PV cell curve tracer are main components of solar simulator. Metal halide lamp has been used in this simulator to provide the light matched to sun light. Ellipsoidal reflector as a concentrator has been designed based on laws of reflection and optical performance parameters .It ensured homogeneous distribution of minimum light intensity of 1000W/m^2 and maximum of 1800W/m^2 at targeted area. Intensity at targeted area was measured by performing calorimetric experiments on aluminum 1100 plate (4cm x 4cm) integrated with engineering designed flux measuring system (FSM).Commercial spectrometer has been utilized to make comparison of spectrum of sun light and simulator. Results show that how close are both spectrums. PV cell curve tracer of solar simulator plots the power output and current-voltage curves of PV cell by interfacing electrical circuit devices with Arduino thus make it easy to quantify the performance effectively. In this way all desired objectives of simulator has been achieved successfully. Simulator has also capability to provide suitable setup and enough space to incorporate cooling mechanism on PV cell and perform study for increase in efficiency and power output .In this way along with primary testing of PV cells, advance studies can also be done with help of this simulator. Moreover the high flux output can be put into use by performing experiments related to concentrated energy phenomenon such as chemical reactions, optical melting of salts, and thermal degradation of materials.

PREFACE

It is great honor and occasion for us to be graduated as **Bachelor** of **Mechanical Engineering** from School of Mechanical & Manufacturing Engineering (SMME), NUST. This report on final year project titled as, "*Design and fabrication of a solar simulator*" is being submitted in partial fulfillment of requirements for degree of **Bachelors** of **Mechanical Engineering** at **SMME**

Every possible effort has been made to complete the project within time allocated using technical knowledge, non -technical skills and resources available. As a result of these efforts, first we have gone through designing phase of project and then on basis of these results, manufacturing of the project has been done. In this way, we presented the working set up of solar simulator to project committee and project has been approved.

Report has been prepared based on research work and manufacturing of project. Report is result of input and work of all team members of the project.

Authors are also indebted to numerous people in presenting work in this report. Special thanks to project supervisor, Dr. Muhammad Sajid and project coordinator Mr. Hafiz Abd Ur Rehman whose views and guidelines have influenced the topics and way of presentation of these topics in this report. In addition, our class fellows and other university fellows helped out in different sections of report. We are thankful to all of them.

ACKNOWLEDGMENTS

All praises to, our creator, Allah, who helped and guided us to complete this project successfully. Without His mercy and blessings we would not be able to complete this project.

We like to express our gratitude to our project supervisor, Dr. Muhammad Sajid, for his patience guidance, enthusiastic encouragement and useful critiques of this work. With his assistance and professional supervision we completed our project successfully and timely.

Our grateful thanks are also extended to Dr. Emad Uddin, Hafiz Muhammad Abd ur Rehman, Engr. Vaqas Arshad, Dr. Syed Muhammad Raza Kazmi and to Dr Nosheen Fatima for their valuable support and useful recommendations on this project.

We wish to acknowledge the assistance and help provided by lab engineers and staff of DMRC, especially Mr. Abbas, Mr. Faisal and Mr. Irfan, in manufacturing of project.

The prayers, wishes, cooperation and perpetual assistance of our most beloved family members deserve a special mention. Our parents, siblings and close friends whom we consider to be our family too; comprehending this humongous task would not have been possible without their eternal support and best wishes.

We would like to offer our thanks to class fellows that kept us motivated and helped out in problems. Special thanks to Ahsan Rauf for providing his assistance in 3D printing. Without his assistance we might not be able to fabricate our reflector

We are thankful to everyone who make our life and studying wonderful at SMME.

ORIGINALITY REPORT

We certify that this research and manufacturing work titled "*Design and fabrication of solar simulator"* is our own work. The work has not been presented elsewhere for assessment, yet. The material used from other sources in this project and thesis have been properly acknowledged / referred. Report has been gone through plagiarism assessment. Results of this assessment have been attached.

Signature of Student
Hamza Butt
NUST201306144BSMME11113F

Signature of Student
Muaaz Farooq
NUST201305701BSMME11113F

Signature of Student
Muhammad Abdullah Haroon Shah
NUST201306224BSMME11113F

Plagiarism Report Results

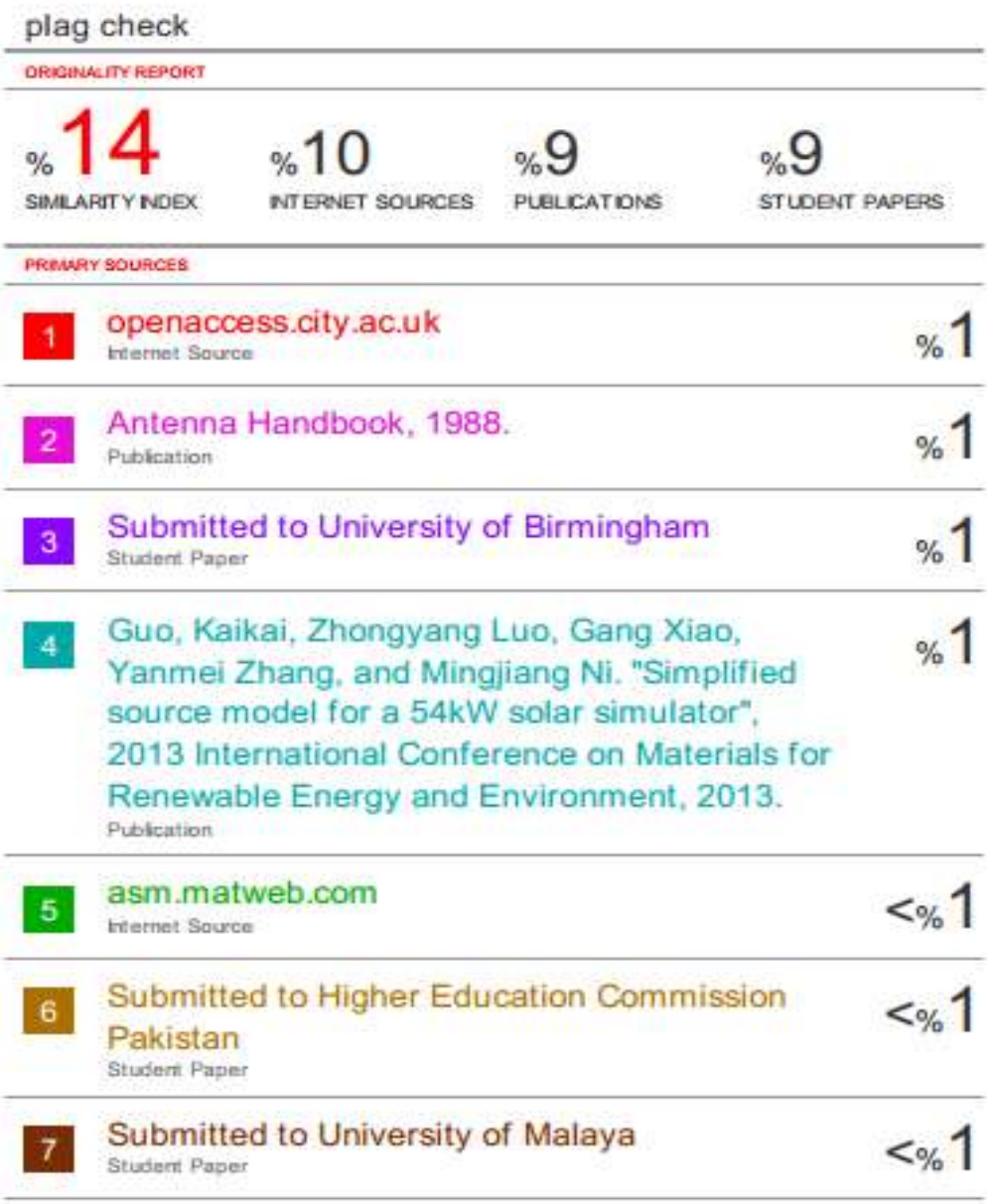

plag check

ORIGINALITY REPORT

%14	%10	%9	%9
SIMILARITY INDEX	INTERNET SOURCES	PUBLICATIONS	STUDENT PAPERS

PRIMARY SOURCES

1	openaccess.city.ac.uk Internet Source	%1
2	Antenna Handbook, 1988. Publication	%1
3	Submitted to University of Birmingham Student Paper	%1
4	Guo, Kaikai, Zhongyang Luo, Gang Xiao, Yanmei Zhang, and Mingjiang Ni. "Simplified source model for a 54kW solar simulator", 2013 International Conference on Materials for Renewable Energy and Environment, 2013. Publication	%1
5	asm.matweb.com Internet Source	<%1
6	Submitted to Higher Education Commission Pakistan Student Paper	<%1
7	Submitted to University of Malaya Student Paper	<%1

Ellipsoidal Reflector and Optical Configuration", Solar Energy, 2005.
Publication

65	K. G. U. Wijayantha. "Twin Cell Technology for Hydrogen Generation", Encyclopedia of Materials Science and Technology, 2008 Publication	<%1

EXCLUDE QUOTES	OFF	EXCLUDE MATCHES	OFF
EXCLUDE BIBLIOGRAPHY	OFF		

COPYRIGHT

TABLE OF CONTENTS

LIST OF TABLES

LIST OF FIGURES

ABBREVIATIONS

PV Photo voltaic

FSM Flux measurement system

NOMENCLATURE

$\boldsymbol{e}$	eccentricity
f	focal length
$2a$	major axis
$2b$	minor axis
d	truncated diameter of reflector
$M1'$	magnified size of arc due to front end of reflector
$M2'$	magnified size of arc due to rear end of reflector
Clc	distance between rear end opening of reflector and focus F1
L	directrix line of ellipse
I	current through load applied across PV cell
V	voltage across load
T	surface temperature of aluminum plate
T_∞	ambient temperature
h	convective heat transfer coefficient
Nu	Nusselt number
Pr	Prandtl number
Gr	Grashof number
Ra_{Lc}	Raleigh number
$\boldsymbol{\sigma}$	Stefan-Boltzmann constant
v	kinematic viscosity of air
k	thermal conductivity of air
α	absorptivity of aluminium 1100
$\boldsymbol{\varepsilon}$	emissivity of aluminium 1100
q_{in}	total heat flux falling on aluminium plate of FSM
$q_{radiation}$	radiative flux leaving aluminium plate
$q_{free-convection}$	convective heat flux leaving aluminium plate
$q_{reflected}$	flux reflected back into space

CHAPTER 1

INTRODUCTION

Solar simulator is the multipurpose device used to simulate the sun light in lab for number of research studies. Research studies includes photo voltaic (PV) cell testing, concentrated solar power testing on materials, chemical reaction studies and biological processes, to name a few.

In this final year project, we aimed primarily to design and fabricate the solar simulator for testing performance of single mono crystalline silicon photo voltaic (PV) cell [40 mm by 40 mm in size] in terms of its efficiency and output with respect rise in temperature. To quantify the performance of PV cells under different high temperatures above the standard operating temperature of 25° C solar simulator would provide reliable environment of necessary and required conditions for PV cell testing. The additional feature of this solar simulator is its capability to facilitate the study of different cooling techniques for negating the effect of heating and improving its performance. In this way different type of studies related to PV cells would be done easily

Organization of report

This report is organized into five different chapters and two appendices.

Chapter 1: Introduction

Explains the title and objective of the project and organization of project.

Chapter 2: Literature review

This chapter summarizes literature review that has been carried out in this regard. It includes need of renewable energies, problems with PV cells, remedies of these problems, work carried out to design different simulators and need of our solar simulator.

Chapter 3: Methodology

Explains the method of designing and fabricating the different components of solar simulator.It includes details of the selection criteria of light, performance parameters of reflector, approach to measure intensity distribution and over all complete fabricated assembly of solar simulator.

Chapter 4: Results

Explains the outcomes achieved during the project. Results include spectrum of light of solar simulator, its comparison with light of sun, intensity distribution and I-V curves of PV cell. Assessments of results have also been made based on outcomes achieved and desired objectives.

Chapter 5: Conclusion and recommendation

This chapter concludes the project. Future prospects of this project based on results have also been presented in this last chapter

Appendix A: Derivations of relations for ellipsoidal reflector

This appendix contains the derivations of analytical relations between geometric variables of reflector based on laws of reflection and trigonometry. These relations lay the foundation of getting best suited values of geometric design of reflector to meet requirements.

Appendix B: Arduino code for data acquisition

This appendix contains Arduino code for acquiring data from PV cell and flux measurement system (FSM).

.

CHAPTER 2

LITERATURE REVIEW

This chapter summarizes the literature review that has been conducted. Literature review is related to need of renewable energy, technologies commonly used for harnessing solar energy , problems of these technologies , remedies of these technologies , need of solar simulator and work carried out in this regard .

Global energy consumption is increasing day by day. Although the primary non-renewable energy resources such as oil, natural gas and coal are contributing largely to the energy requirements. But these resources are limited. With the current rate of consumption, these resources will last only a few more decades. Thus to decrease the dependency on non-renewable resources many countries are trying to harness different energy renewable energy resources. Consequently in a short period of few years, rapid increase in share of renewable energy to global energy consumptions has been observed all over the world. By the year 2006, the renewable technologies were supplying 13.3 % of global energy consumption and rose up to 19 % in 2011. During the period from 2007-2012, out of all renewable energy sources average annual growth rate of solar energy capacity remained higher globally[1]

Commercially crystalline silicon cells are being used far and wide to meet the growing energy requirements. In the commercial market worldwide crystalline solar cells hold the predominant shares (80-90%) while thin films mainly occupy the remaining shares. Although crystalline silicon cells are difficult to manufacture their efficiency is high as compared to other cells. Within the category of crystalline silicon cells, mono crystalline are used extensively than poly crystalline silicon cells. The mono crystalline cells have better efficiency over poly crystalline cells that compensates the high cost of these cells .The claimed efficiency of mono crystalline cells by manufacturers lies between 14-17% [2, 3].Mono crystalline cells with efficiency range of 17-24% have also been reported but being costly, difficult to manufacture and under research, there market availability will take time.[4, 5]

There are number of factors that affect performance of crystalline silicon cells .The temperature has major impact out of all these factors .The efficiency and electrical output degrades with rise in its operating temperature [6-8]. The conversion efficiency drops by around 0.4 - 0.50 % with every degree rise in temperature above 25 °C [3, 4, 9].It dictates us to maintain temperature as close as to 25°C for good performance but due to low inherent efficiency the major portion of incoming solar energy is dissipated as heat within cells and temperature increases[10, 11]. It has been observed in different experimental studies that under intense solar radiations for long durations and without proper cooling mechanisms temperature of silicon cell increases even up to 70 °C .This results in large losses in cell efficiencies [12-18]. In long run, the high temperature also causes thermal stresses in silicon cells.

Increase in energy demands and low efficiency of PV cells should at higher temperature is matter of concern for both producers of these PV cell technologies and consumers. Different types of studies are being conducted in this regard. Most of researchers all over the world are testing the solar cells for extended periods of time under direct sunlight and then employing different cooling techniques to negate the heating effect thus developing the performance coefficients of PV cells. On the other hand, PV cell industries are working to make these cells to work efficiently in harsh environments.

In both these kinds of studies, a reliable environment is required that should provide necessary and desired conditions for testing. But however in most of the studies, direct sunlight has been used to test these cells for thermal behavior [4, 12, 13, 19, 20].Though outdoor environment is reliable to much extent in terms of sunlight properties but due to present conditions of environment, it is matter of risk and laborious task to wait for proper sunshine and clear day for testing of PV cells. Secondly environment conditions are time dependent and one can work only when there is proper sunlight and clear sky. For making the studies these experiments to be implemented in the industries and fruitful then the testing environment should be control able and reliable just like laboratory conditions. Such environment is provided by the designed solar simulator.

In most of studies of solar simulator design that has been found during this literature review, main objective was to focus characteristic sunlight on very small areas and to

produce high thermal flux at the targeted area. The purposes of these solar simulators was to study advanced high-temperature materials, chemical reactions with high intense radiations, optical melting of salts, thermochemical, and concentrated solar power studies for power production .In most of the designs where targeted area was relatively small, xenon and metal halide lamps were used to spectrum match of sun with ellipsoidal reflector as concentrator. For performance characterization of solar simulators spectrum, intensity distribution and efficiency of solar simulators were measured using calorimetric techniques, spectrometers and flux gages [21-26] .

Qinglog and his co-fellows designed a solar simulator that was in line Class B of the ASTM (American Society for Testing and Materials) and IEC (International Electro technical Commission) standard in regard to spectrum match, irradiance uniformity and stability. This multi lamp solar simulator can provide average irradiance on the target area between 150 and 1100 W/m^2 [27].

Through literature review we come to point that we should make use of either metal halide or xenon lamps as light source and ellipsoidal reflector as concentrator .Because these lamps provide light that is very close to sun light in its properties and ellipsoidal reflector provides uniform intensities of light over small area just like a single silicon cell.

It has been observed that large number of solar simulators have been designed for providing high flux of nearly uniform intensities by using large number of xenon and metal halide lamps with ellipsoidal reflectors as concentrator. In some designs Fresnel lens and other techniques have also been used[28] for studying different thermal energy based process .

Very few simulators have been found that were simple and cheap and designed solely for PV cells testing. Large number of lamps with large number of concentrators were employed in most of these designs.On the other hand, by using single or small number of lamps, a simple solar simulator can be designed and fabricated with the aim to test PV cells. Thus it will be a relatively cheap simple and a new kind of simulator as compared to high flux solar simulators. This solar simulator would be available locally to both students and industries for research studies on PV cells

CHAPTER 3

METHODOLOGY

This chapter describes approach that has been undertaken during the project for designing and fabricating solar simulator and its outcomes. Approach is based on the objective of the project, that is, solar simulator must provide necessary and standard conditions for testing the performance of single mono crystalline photo-voltaic (PV) cell, the components/systems of solar simulator to achieve these necessary and standard conditions and availability of manufacturing resources.

Following details have been narrated in this chapter in regard to required solar simulator.

A) Main headings:

3.1 Necessary conditions for testing of mono crystalline silicon PV cell.

3.2 Components/systems of solar simulator

3.3 Design and fabrication of components /systems of solar simulator

3.4 Complete solar simulator assembly

B) Sub headings:

3.3.1 Light source

3.3.2 Concentrator

3.3.3 Data acquisition systems/devices

3.3.4 Metallic frame and other accessories

3.1 Necessary conditions for testing of mono crystalline silicon PV cell.

1. Homogeneous irradiation on testing plane
2. Incident light should have flux of about 1000 W/m^2 (this is equal to one sun).
3. Spectrum of artificial light source should be close enough to spectrum of sun light.

3.2 Components/systems of solar simulator [1]

Solar simulator is comprised of following components and systems to achieve

1. Desired conditions for PV cell testing discussed.
2. Performance curves of PV cell and plot the curves for further usage.

- **Light source**

  This light source provides light that have characteristics of sunlight and suitable for testing of PV cell.

- **Concentrator**

  Reflector is needed to provide the parallel rays of light with uniform intensity over a small area .In this small area, a single mono crystalline silicon PV cell, and data acquisition devices will be placed .PV cell, in this project have square shape with each side equal to 40 mm.

- **Data acquisition systems /devices**

  For characterization of solar simulator data acquisition devices are required. Characterization of solar simulator is measure of its performance .These devices are used to measure the extent up to which solar simulator is capable of providing necessary conditions for PV cell testing .Thus we have following devices/systems serving the specified purposes.

  a) **PV cell curve tracer system**: Tracing current-voltage and power-voltage curves with change in temperature of PV cell .These curves are indicator of change in performance of PV cell with temperature

  b) Light spectrometer: To measure the spectrum of light being focused by reflector on to the cell .This device provides means to match solar simulator light spectrum with standard sun light specter thus enables us to explain how good our solar simulator is in achieving the desired spectrum.

[1] Details of each component has been presented under heading 3.3

c) Flux measurement system: To measure the flux of light being focused on to the cell. Flux measurement of light is necessary as it will shows whether the solar simulator is providing the right flux (1000W/m^{2} = 1 sun) or not.

- **Metallic frame and other accessories**

  Metallic frame holds all components and devices at required positions with respect to each other to achieve the desired results .The metallic frame also provides the opportunity to move solar simulator from one point to another. Accessories includes cooling fans, metallic strips, wooden walls to cover the sides of reflector and glass wool for heat insulation.

3.3 Design and fabrication of components /systems of solar simulator

Few components of solar simulator has been selected according to our requirements and then bought and few components has been completely designed and fabricated from scratch.

Following components has been selected and bought

1. Light source and its power supply accessories
2. Light spectrometer
3. Exhaust fan and cooling fan

Following components has been designed and fabricated

1. Reflector
2. Flux measurement system (FSM)
3. Metallic frame to hold all components at relevant positions
4. PV curve tracer

3.3.1 Light source

The intensity of light from the sun varies greatly depending upon position and weather conditions. For the laboratory testing purposes a light source which could produce repetitive results. A homogeneous light source was needed which has a similar light spectrum to the sun. A uniform light source of homogenous spectrum was required which could serve as a substitute for sunlight. An artificial light source was required which would meet the light source standards for solar simulators. Light source should be capable of [29]:

- Simulation of average global radiation according to **AM 1.5 spectrum** as shown in Figure 1.
- Irradiation of about 1000 W/m2 (this is equal to one sun) adjustable.
- Homogeneous irradiation on testing plane.
- Time continuous irradiation on testing plane.
- Low divergence angle of irradiation.
- A light source equivalent to a black body with temperature around 5500K.

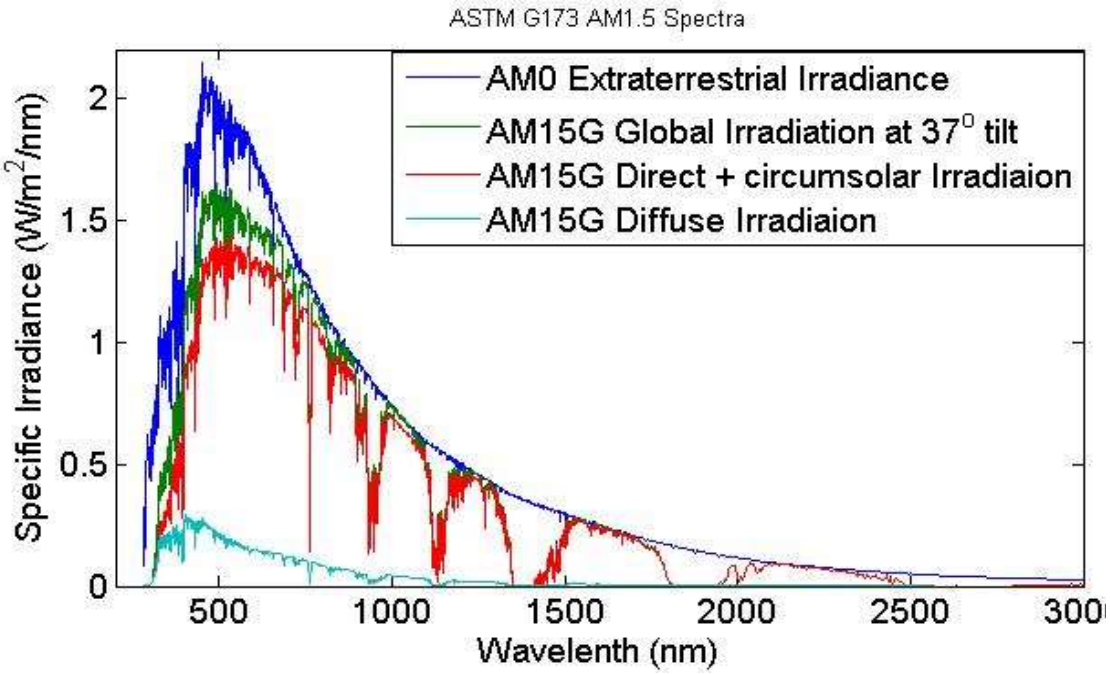

Figure 1: AM 1.5 Solar radiation spectrum

3.1.1.1 Classes of Light sources

Different sources of light are classified according to parameters such as spectral match, non-uniformity and temporal stability. All these parameter combined tell us how much comparable the light source with respect to the sun. According to these parameters, the light sources are divided into sub classes as shown in Figure 2.

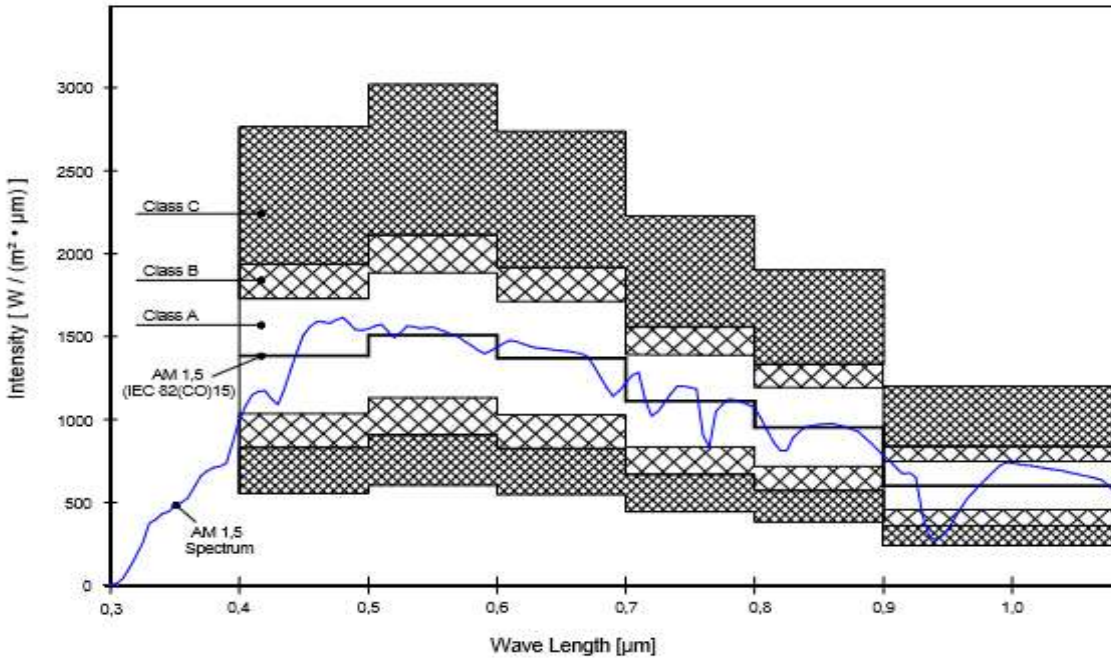

Figure 2: AM 1.5 Spectrum and bandwidth of simulator class A,B and C according to IEC 82 (CO) 15

3.1.1.2 Light sources discussed in literature

A number of light sources have been discussed by researchers for solar cell testing. Atkin at al., 2015[30] used two 500W halogen lamps positioned 0.15 m away from the center of each solar panel, which gave a peak insolation of 920 W/m^2. Maiti et al., 2011[31] incorporated a tungsten halogen lamp of Philips make rated at 1000 W. Ebrahimi et al., 2015[32] integrated three 400W metal halide lamps to replicate solar radiations. For emulating solar radiations Karami et al.,[17] used three metal halide lamps and maintained a constant irradiation of 1000 W/m^2 throughout the experiment. Al-Shohani et al.,[33] also used a metal halide lamp for producing a light intensity of 1000W/m^2 at room temperature of 25 °C with maximum tolerance of ±20W/m^2.

A review of industrial solar simulators was also done and by comparing the data available commercially and in literature following three light sources were selected.

- Xenon lamp
- Halogen lamp
- Metal halide lamp

3.1.1.2.1 Xenon Arc Lamp

Xenon arc lamps belong to Class A radiation sources (as previously mentioned). They give the closest radiation spectrum with respect to sun. A number of commercially available solar simulators use xenon lamps as a radiation source. Xenon arc lamps are not locally available in Pakistan and for our requirements a minimum of 1000 W lamp was needed whose price comes according to the online stores at about 50000 PKR for one 1000 W lamp. If we were to select a xenon arc lamp it would have had to be shipped from abroad. If we include the price of the power supply (which is a little expensive as well) and the shipping costs it comes around to 70000 PKR. The Figure 3 gives a radiation spectrum graph of xenon arc lamp[25].

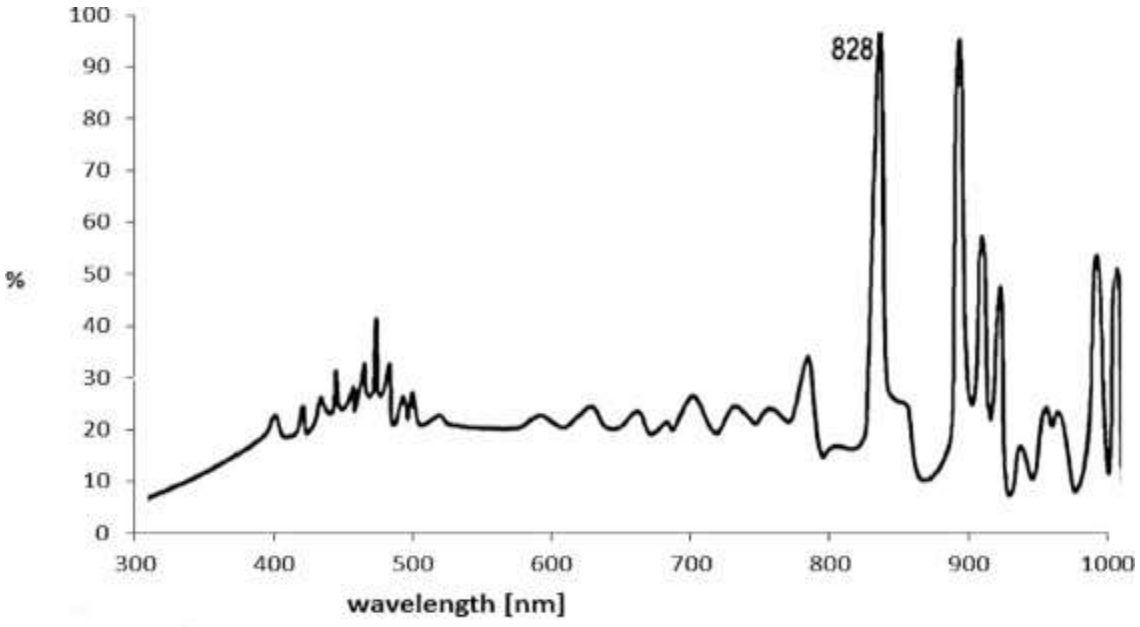

Figure 3: Spectral distribution of radiant energy emitted by the xenon lamps

3.1.1.2.2 Halogen Lamp

Halogen lamps belong to Class C radiation sources (previously explained). Halogen lamps are available only for a color temperature of **3300 K**. Halogen lamps give two types of spectrums a small range spectrum of visible region and a major spectrum range in the infrared region. Halogen lamps were locally available but according to the market survey done halogen lamps were of low light intensities. The maximum 1000W lamp available had a luminance of 16000 lumens. To get the required light intensity of one sun (1000 W/m^2) approximate seven 1000 W halogen lamps would have to be used. But as the number of light sources increases the uniformity of light spectrum decreases.

3.2.1.2.3 Metal Halide Lamp

Metal halide lamps are class B radiation sources (previously explained). Metal halide lamps are available for a color temperature range of 5500-6000K .Lamps ranging from 100-1000 W are available in the market. The price of a 1000 W metal halide lamp according to the market survey was 13500 PKR (including the power supply). The following graph in Figure 4 shows the radiation spectrum of a metal halide lamp[25].

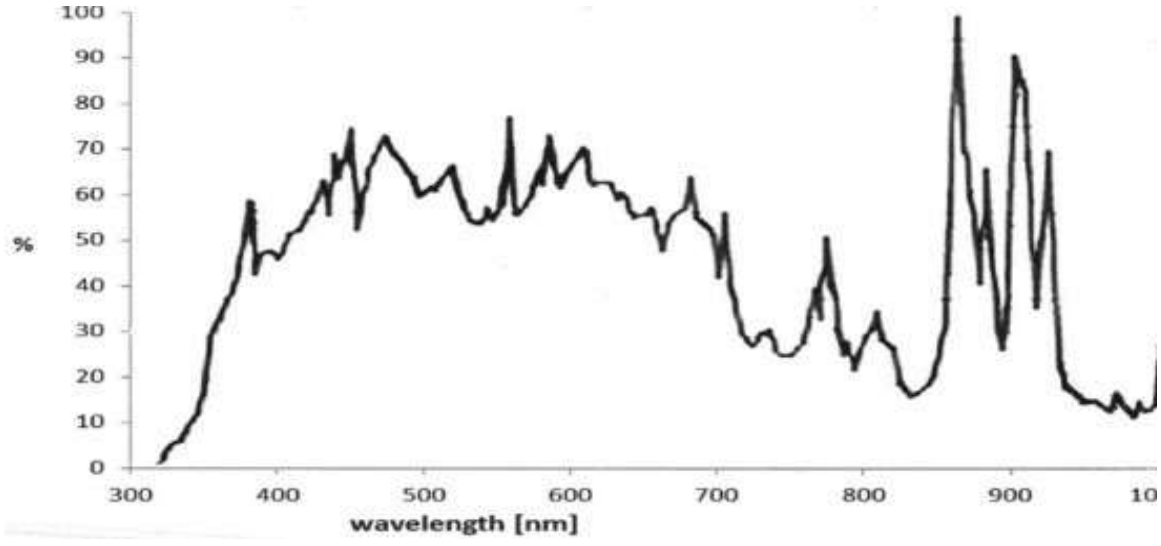

Figure 4: Spectral distribution of radiant energy emitted by the metal halide lamp**.**

After reviewing all the available light sources and considering the spectrum, light intensity, color temperature and market availability, metal halide lamp of rated power 1000W was chosen as shown in Figure 5

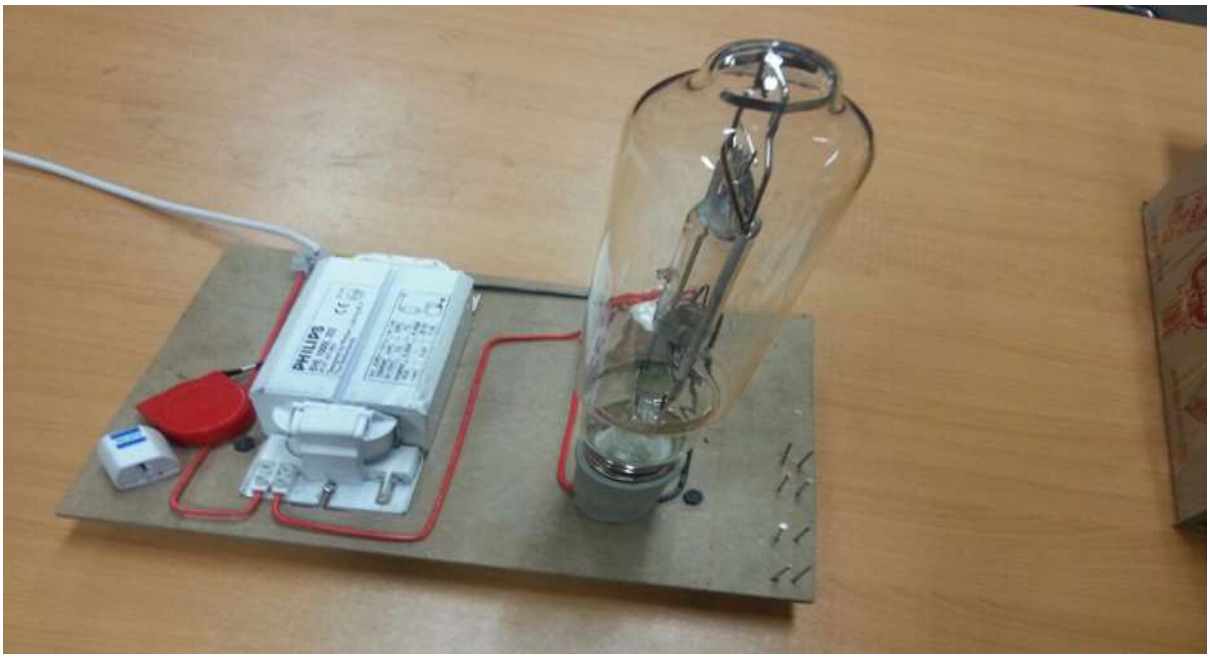

Figure 5: 1000 W Metal halide lamp and power supply

3.3.2 Concentrator

Concentrator in solar simulator plays a major role in achieving the conditions for PV cell testing. Concentrator in this solar simulator have been designed with the aim to achieve the followings

1. To provide the parallel rays of light with uniform intensity over a small specified area. In specified area, a single square shaped PV cell with each side equal to 40 mm, a small spectrometer and a small flux measurement device will be placed

2. To provide light flux of 1 sun (1000W/m^2) at least on to the specified area.

3. For maximum utilization of light of the lamp that was being wasted by spreading in all directions

3.3.2.1 Ellipsoidal reflector as a concentrator

Type and design of concentrating system depends on the type of activity, results needed, resource availability and ease of using these devices. The most commonly used geometrical designs of concentrators are parabolic troughs, compound parabolic concentrators, flat and ellipsoidal reflectors. Fresnel, convex, concave and other different lenses are also used with theses concentrators [23, 25, 26, 28, 34, 35].The concentrating system used commonly for focusing light on small area such as area of single solar cell size with parallel ,high and uniform intensity is ellipsoidal reflector[21-23, 25]. In this system a single ellipsoidal reflector is used. Ellipsoidal reflector is surface of revolution. It is formed by revolving planar ellipse (conic section) about its major axis. When a point source of light is placed on one of foci F1, the light rays after reflection converge to second focus F2.Thus by placing light source at one focus and target area at second focus, light can be concentrated on the target area as in Figure 6 .

3.3.2.1.1 Basis of Selection of Ellipsoidal Reflector as Concentrating System

Following key points make the ellipsoidal reflector suitable to work as concentrating in this project.

1) Offer high efficiency radiation transfer compared to others reflector as by placing point light source at focus F1 then after single specular reflection must reach second focus F2.

2) It provides axis symmetry flux distribution (radially uniform flux about focus F2 when point light source is placed at F1)

3) It focuses light to a single point thus making it suitable for our small targeted area of focusing light

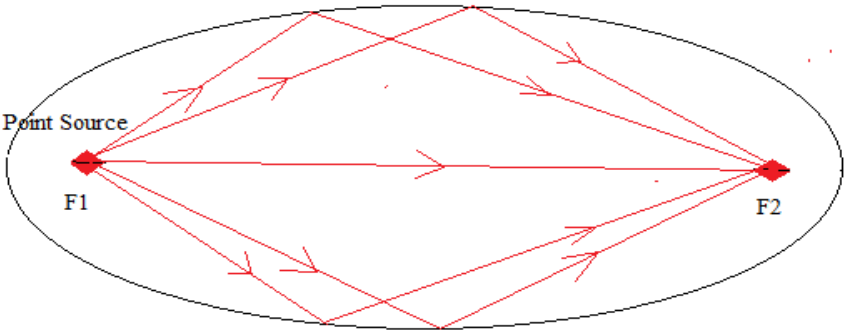

Figure 6: Ellipsoidal reflector with point source of light

3.3.2.1.2 Optical Performance Parameters

Followings are the optical performance parameters. These parameters effect the optical performance of ellipsoidal reflector. These parameters are strongly dependent on the geometric construction and size of light source

1. **Exchange factor** In practice ellipsoidal reflector does not perform well as theoretically. It is due to the finite size of light source .This light source is magnified after reflection and in this way light does not reach specified target thus effecting the reflector radiation transfer efficiency .To quantify this effect exchange factor is defined for reflector .It is defined as the defined as the fraction of diffuse energy leaving a surface that arrives at a second surface both directly and by all possible intermediate specular reflections[36].In studies it has been shown that smaller the eccentricity and smaller the light source size, larger will be the exchange factor[37].

2. Specular errors Reflector surfaces do not have smooth and plane surfaces .Their surfaces cannot be plane and smooth as we assume in theory. So image formed through these reflectors get blurred .This blurriness depends on the surface and focal length of ellipsoidal reflector .For longer focal lengths these errors in image get magnified and image goes on more blurry .Thus small focal length is recommended. But due to relatively large lamp size and heat produced by lamp the focal length is kept to a safe value. Lower focal length at fixed eccentricity makes the rear end reflector closer to the light that may cause damage to coating and also make the ventilation difficult.

3. Radiation intercepted by reflector practically the complete closed ellipsoidal surface is not used, however it is truncated at angle. The effect of angle at which the reflector is truncated on performance of reflector is not significant, and therefore in design the angle is kept to be 60° .The truncation diameter ***d*** has effect on performance of reflector. The larger the truncation diameter, more rays are intercepted by the reflector, and as result more rays are reflected to second focus F2.Thus efficiency of reflector is increased at larger truncation diameter. Efficiency (ɳ) is defined as ratio of energy reaching at target *ė* to ratio that has produced at source *Ė[22]*

$$\eta = \frac{e}{E}$$

Following figures highlight the above discussed performance parameters

Figure **7 shows the planar ellipse with its geometrical variables:** Foci of ellipse lie on major axis (***2a***). Major axis ***(2a***) and focal length ***(2c***) are related to each other through eccentricity e as

$$e = \frac{c}{a} \tag{3.1}$$

And minor axis (**2b**) is related to major axis as

$$b = \sqrt{a^2 - c^2} \tag{3.2}$$

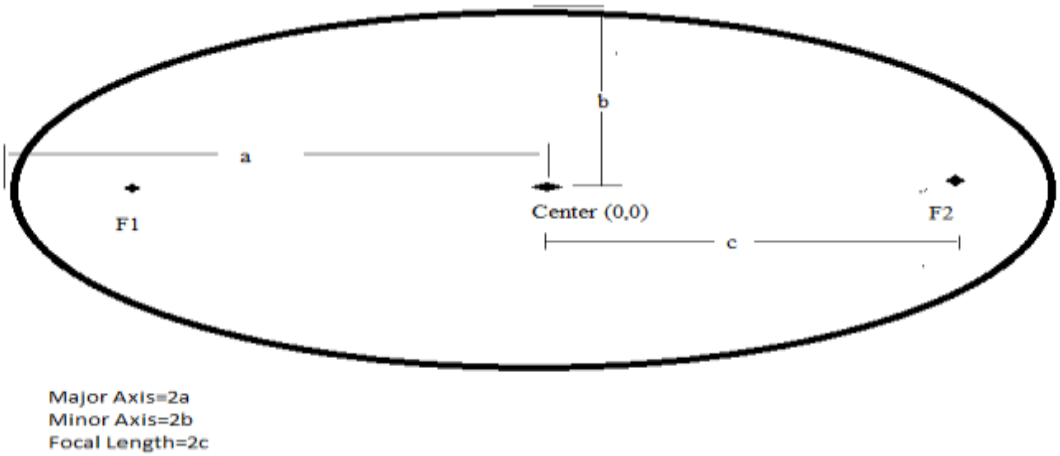

Figure 7: Planar ellipse

Figure **8 shows the truncated reflector** the diameter of this truncated section is called truncated diameter (d). The rear end of reflector is opened to place the light source with whole size of ***2h.*** The lightning element (origin of light) within metal halide lamp is an arc of finite length. Thus light source is placed length wise along major axis in such manner that midpoint of arc coincides with focus say F1.

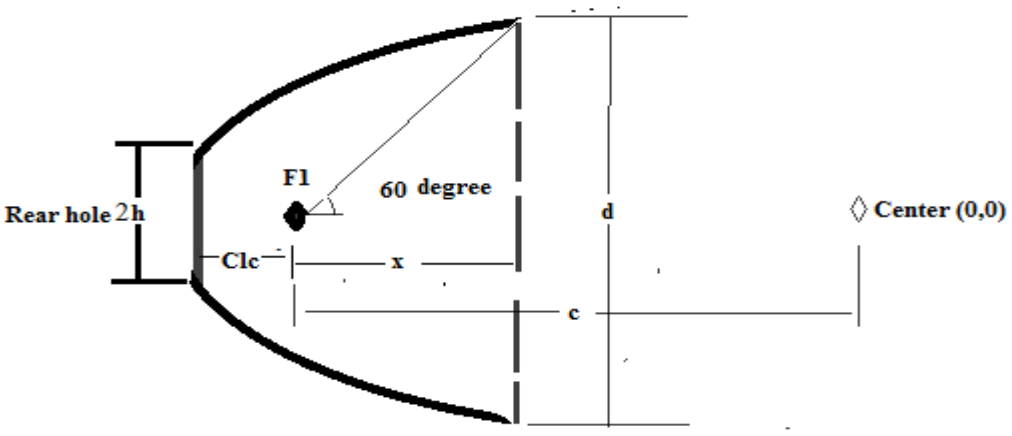

Figure 8: Reflector truncated at angle of 60°

Figure 9 and Figure 10 shows the magnification of arc after reflection

Arc size in metal halide lamps is of finite length, which after reflection magnifies to a certain level depending upon the size of arc and eccentricity. Lamp is placed in such a way that arc midpoint coincides with focus ***F1.*** Right end of reflector gives the minimum magnified size ***M1´ (double of M1)*** and left end maximum magnified size ***M2′(double of M2).***These magnification were determined through laws of reflection

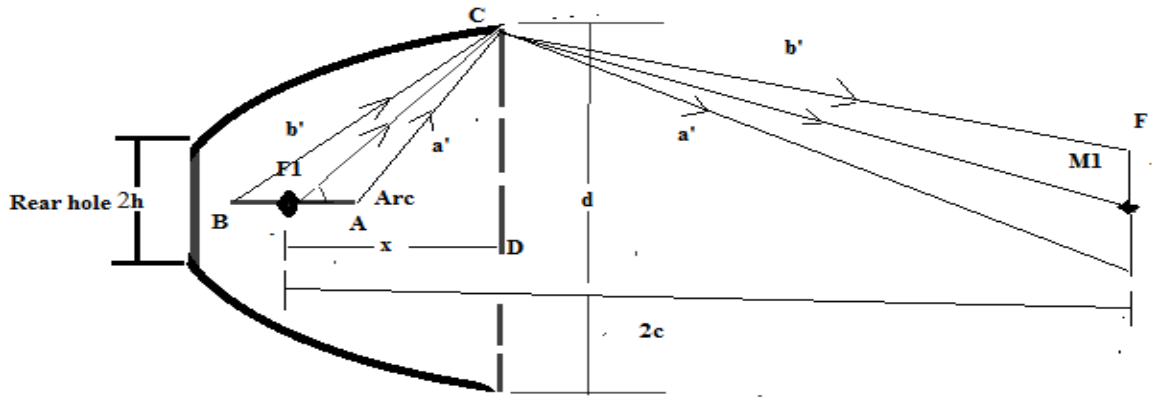

Figure 9 : Half of arc magnified size , M1 due to right end of reflector

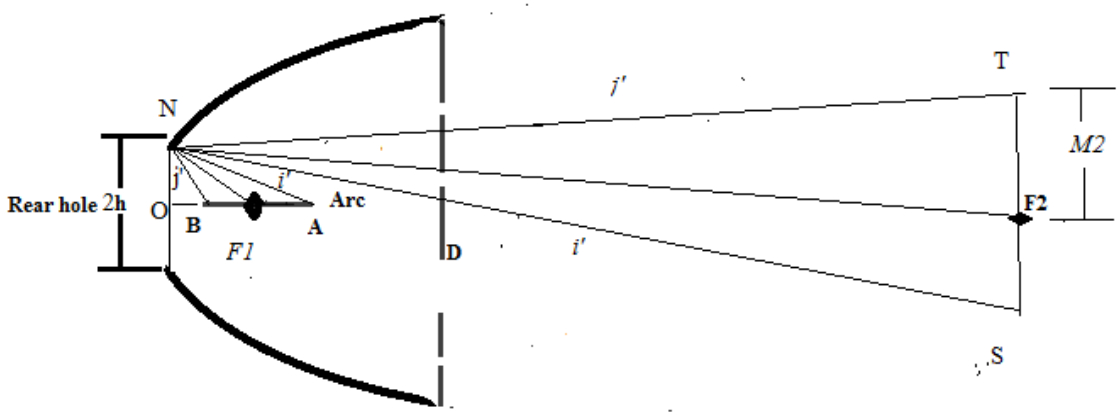

Figure 10: Half of arc magnified size ,M2 due to rear end of reflector

3.3.2.1.3 Designing of Reflector

Arc size, eccentricity *e*, truncated diameter *d*, focal length *2c*, and distance between the rear end opening and focus F1 (*Clc)*, effect the optical performance parameters of reflector. Figure 10 shows these geometric variables.

Approach to get best suited values

Best suited values of theses variables will determine the performance of reflector. Commercial soft wares are available that are used to get optimum values for given constraints. We did not go for commercial soft wares however on the basis of laws of

reflection and given data analytical relations has been developed and then on basis of these relations best suited values of geometric parameters were defined

1. Relationship between geometrical variables[2] .See Figure 11

We have independent variables as:

a) Eccentricity e

b) Focal length 2c

We have dependent variables

a) Truncated diameter d

b) Arc Magnified sizes M1´ and M2´

c) Distance between focus F1 and rear end (Clc)

Constants: *Half arc size =42.5mm and Rear end hole =2h=150mm*

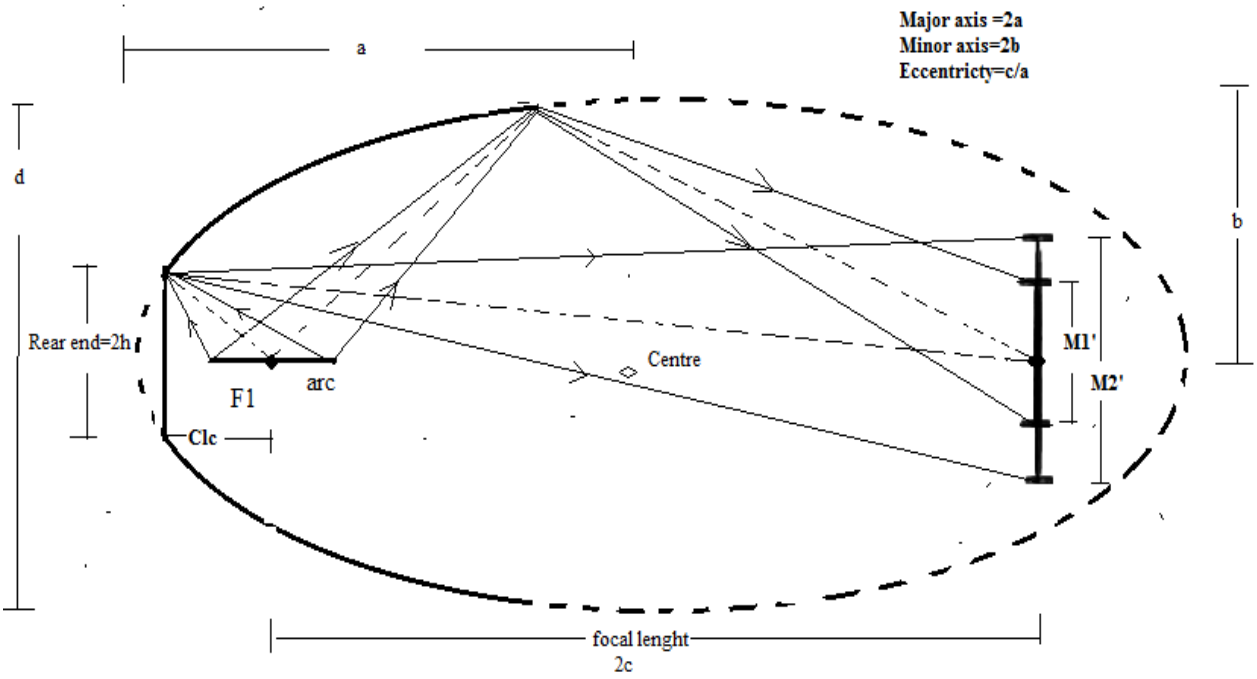

Figure 11: Geometric variables of reflector

[2] See APPENDIX A: DERIVATIONS OF ANALYTICAL RELATIONS FOR REFLECTOR

Thus following relations were define using laws of reflection and trigonometry

A) Arc Magnified Size *M1´ (mm)*

$$M1 = \frac{d}{2} - \frac{2c - 0.2886d}{tan\left(\frac{\Phi'}{57.295}\right)} \quad \text{(A.7)}$$

$$M1 = 2M1 \quad \text{(A.8)}$$

Where

$$\Phi'(degree) = 57.295\ tan^{-1}(4c - 0.5773) + \gamma \quad \text{(A.6)}$$

$$\gamma(degree) = \frac{(\alpha - \beta)}{2} \quad \text{(A.5)}$$

$$\alpha(degree) = 57.295(tan^{-1}\ \frac{x - 42.5}{d/2}) \quad \text{(A.3)}$$

$$\beta(degree) = 57.295(tan^{-1}\ \frac{x + 42.5}{d/2}) \quad \text{(A.4)}$$

$$x(mm) = 0.28867d \quad \text{(A.2)}$$

B). Arc Magnified Size *M2´ (mm)*

$$M2 = h + \tan(\mu)\ (2c + Clc) \quad \text{(A.15)}$$

$$M2 = 2M \quad \text{(A.16)}$$

Where

$$\mu(\text{degree}) = \varphi - \Theta \quad \text{(A.14)}$$

$$\theta(degree) = 57.295tan^{-1}\left(\frac{h}{(2c + Clc)}\right) \quad \text{(A.13)}$$

$$\varphi(degree) = \frac{(\omega - \psi)}{2} \tag{A.12}$$

$$\omega(degree) = 57.295 tan^{-1}\left(\frac{Clc + 42.5}{h}\right) \tag{A.10}$$

$$\psi(degree) = 57.295 tan^{-1}\left(\frac{Clc - 42.5}{h}\right) \tag{A.11}$$

c). Distance between focus F1 and rear end opening, *Clc (mm)*

$$Clc = \frac{-2e(a - ce) \pm \sqrt{4e^2(a - ce)^2 + 4(1 - e^2)(h^2 - (a - ce)^2)}}{2(1 - e^2)} \tag{A.9}$$

2. Inferences from these relations

Based on previous relations following conclusions have been drawn

A). **Diameter d** as function of **eccentricity (e)** and **focal length (2c)**

B). M1′ as function of **eccentricity (e)** and **focal length (2c)**

C). M2′ as function of **eccentricity (e)** and **focal length (2c)**

A). Diameter d as function of eccentricity (e) and focal length (2c)

Analytical relation for **d** could not be found however graphs were drawn by sketching ellipse for each value of focal length and eccentricity in Solid Works. From Figure 12, at fixed **focal length 2c**, **truncated diameter d** increases with decrease in **eccentricity e**. This behavior is in our favor. Because we need larger diameter to maximize the radiation intercepted by reflector. At same time lower eccentricity will give higher exchange factor. However at larger focal lengths diameter also increases

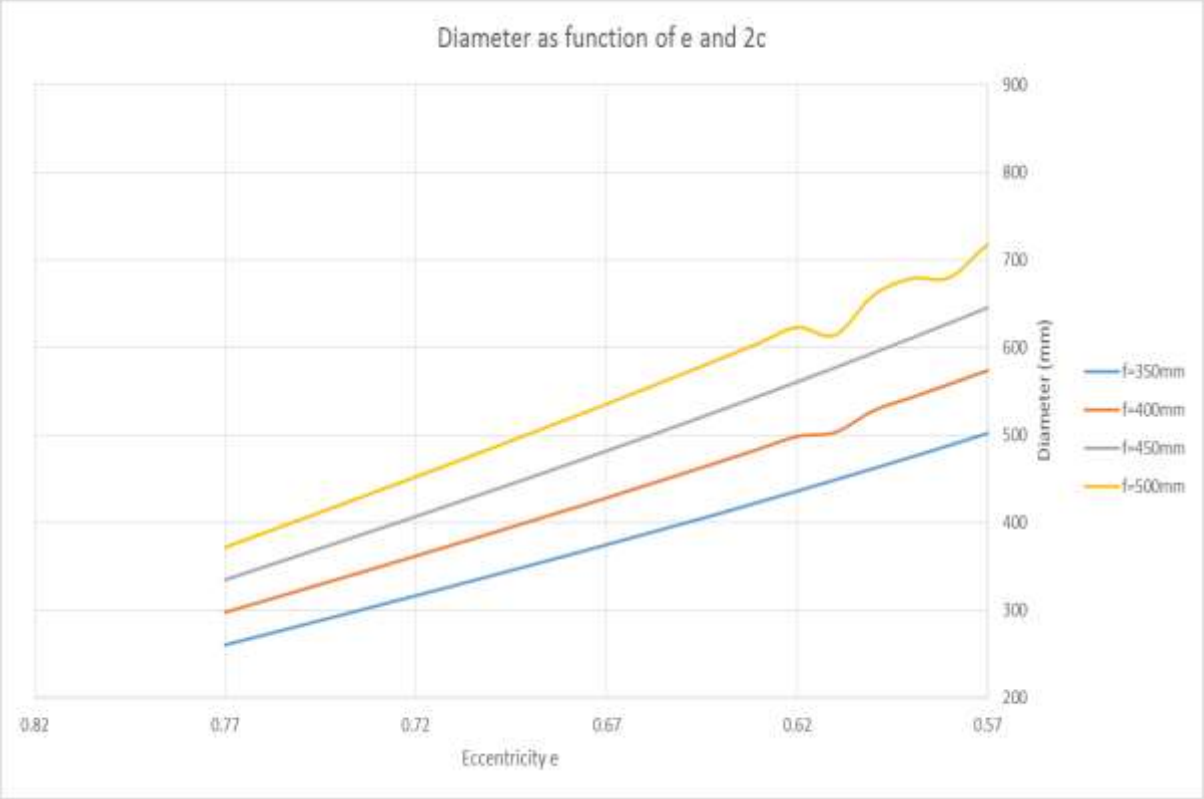

Figure 12: Truncated diameter d as function of eccentricity e and focal length 2c

b) M1′ Function of eccentricity (e) and focal length (2c)

From graph shown in Figure 13.

- **M1′** does not vary significantly with **focal length 2c**
- It first decreases with decrease in **eccentricity e** and then increases with further decrease in **eccentricity e.**
- It suggest to use eccentricity within range of **0.65-0.55** giving low magnified size and higher exchange factor

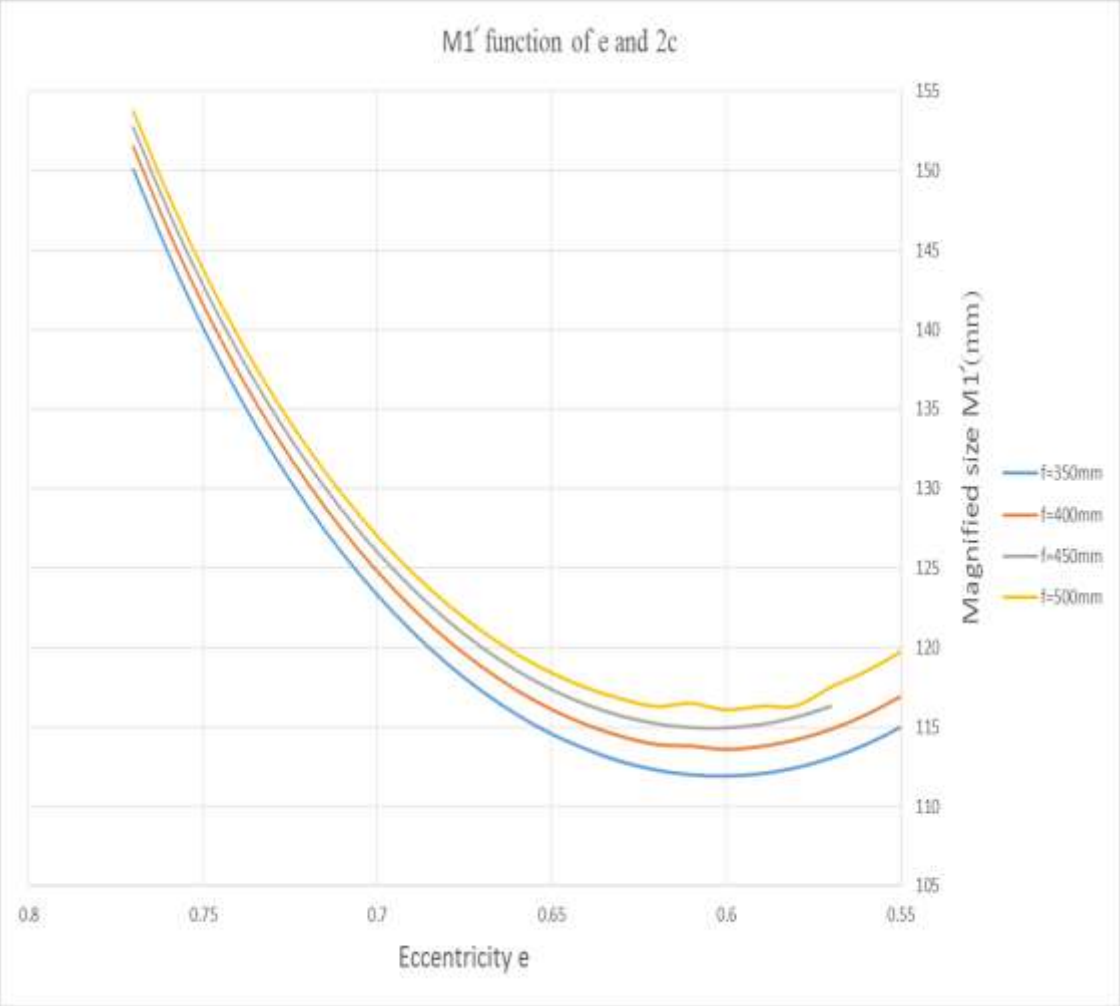

Figure 13: M1′ function of eccentricity e and focal length 2c

C).M2′ as function of eccentricity (e) and focal length (2c)

From graph shown in Figure 14

- **M2′** varies both with **focal length and eccentricity**
- With increase in focal length , it first decreases and then increases
- With decrease in eccentricity it decreases
- It suggest us to use focal lengths of 400mm or 450 mm.

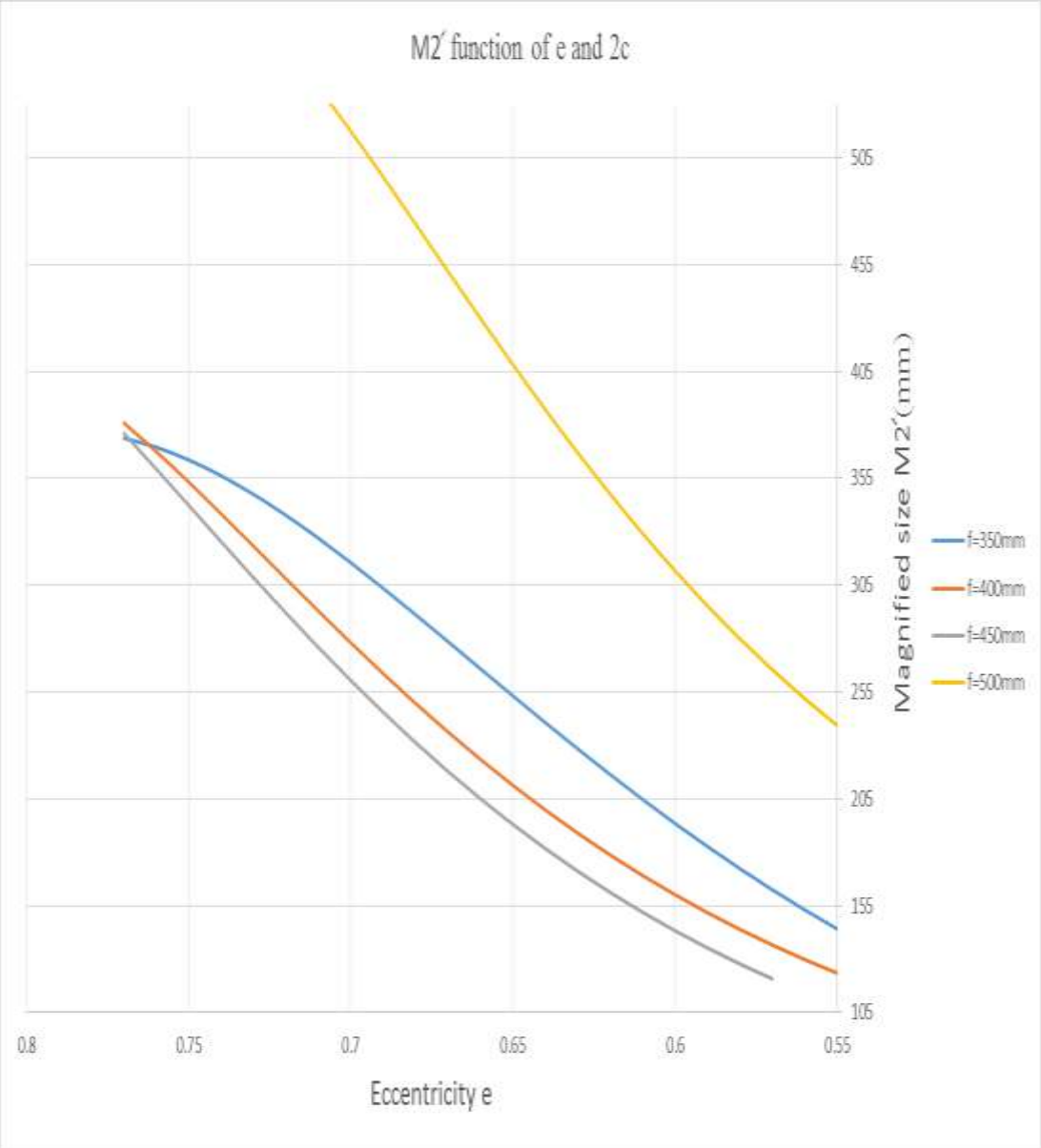

Figure 14: M2′ function of eccentricity e and focal length 2c

3. Final reflector design

We have developed the relations and got inferences from them. Now we are able to find the optimized value of these variables for having best performance parameters. Followings were the constraints in optimizing the values of geometric variables.

Constraints

- Lower eccentricity e for higher exchange factor
- Larger diameter d for intercepting large number of rays
- Maximum diameter can be 483 mm(19 inches) due to manufacturing limitations
- Small focal length for reducing magnification of specular error. But at the same time focal length should be large enough to accommodate the lamp inside reflector and avoid heating problems
- Clearance (Clc) should be more than 100mm.
- Arc magnification should be minimum as possible.

Based on previous relations and constraints, reflector with followings geometrical parameters was finalized

Table 1:Best suited values of geometric variables for reflector

Focal length(***2c***)	450 mm
Eccentricity(***e***)	0.64
Truncation angle	60°
Truncated diameter(***d***)	470 mm
Magnification (***M1´***)	115mm
Magnification (***M2´***)	199mm
Clearance(***Clc***)	105mm
Rear hole size(***2h***)	150 mm

3.3.2.2 Concentrator fabrication

Due to the large truncated diameter and depth of reflector many challenges arose during its manufacturing process. It was difficult to construct it in only one single piece. So the following strategy was employed for reflector manufacturing.

- A quarter portion of the 3d model was printed using a 3d printer, see Figure 15.

Figure 15: 3D printed mold for reflector(Quarter)

- Using casting techniques four identical parts were made using the 3d mold. These four pieces were then joined together and the internal surface was buffed and polished for optimum surface smoothness, see Figure 16.

Figure 16 : Fabricated reflector

3.3.3 Data acquisition systems/devices

For thermal characterization of PV cell and to check whether the solar simulator is providing the desired objectives of project we have followings data acquisition systems and devices.

a) **PV cell curve tracer system**

b) Flux measurement system

c) Light spectrometer

PV cell curve tracer and flux measurement system (FMS) were designed and manufactured while light spectrometer was bought. In following headings, design and fabrication of PV cell curve tracer and FMS has been explained

3.3.3.1 PV cell curve tracer system

A) Basic schematic circuit for current (I) and voltage (V) values

For analyzing the performance of PV cells, the values of voltage and current at various load levels across the PV cell are required. The basic scheme of the circuit is shown in Figure 17.

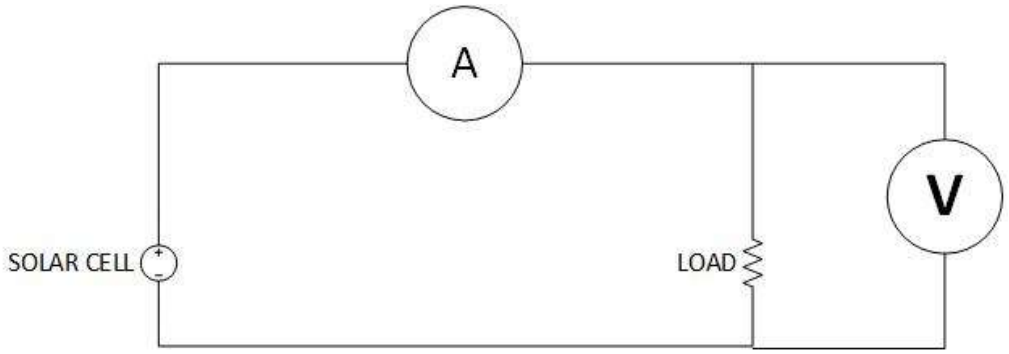

Figure 17 : Basic schematic circuit for acquiring current and voltage of PV cell

B) Designed circuit and data acquisition lay out for tracing performance curves

For this purpose a circuit is required that can automatically vary the load across the cell in steps at regular intervals. An N-channel MOSFET (Metal oxide semiconductor field effect

transistor) was used as a variable load in the circuit. The body of the MOSFET consists of a semiconductor material and is separated from the gate by an insulation layer. The MOSFET consists of gate, drain and source terminals. An N-channel MOSFET has source and drain terminals as n-type doped regions while the body is a p-type doped region. When a voltage is applied at the gate terminal of the NMOS the gate to body voltage V_{GB} increases and a depletion layer is created, when the voltage is further increased to the point where the concentration of electrons and holes is equal, it is called threshold voltage. Increasing the voltage further increases the Gate Source voltage and the transistor starts to conduct current. The voltage above the threshold voltage is termed as excess voltage. Above the threshold voltage the MOSFET behaves as a linear transistor in the triode region. When the Drain Source voltage exceeds the excess gate voltage the MOSFET enters the saturation region and current increases at a high rate. Using this concept a MOSFET in its triode region can be used as a variable load across the PV cell.

The values of current, voltage and power with respect to varied loads were acquired through a circuit that varies the load across the cell by the use of an N-channel MOSFET (NMOS). The MOSFET utilized was modelled FQD30N06. In this way, by varying voltage at the gate, a load is induced across the PV cell. The schematic of the designed circuit is shown below in Figure 18.

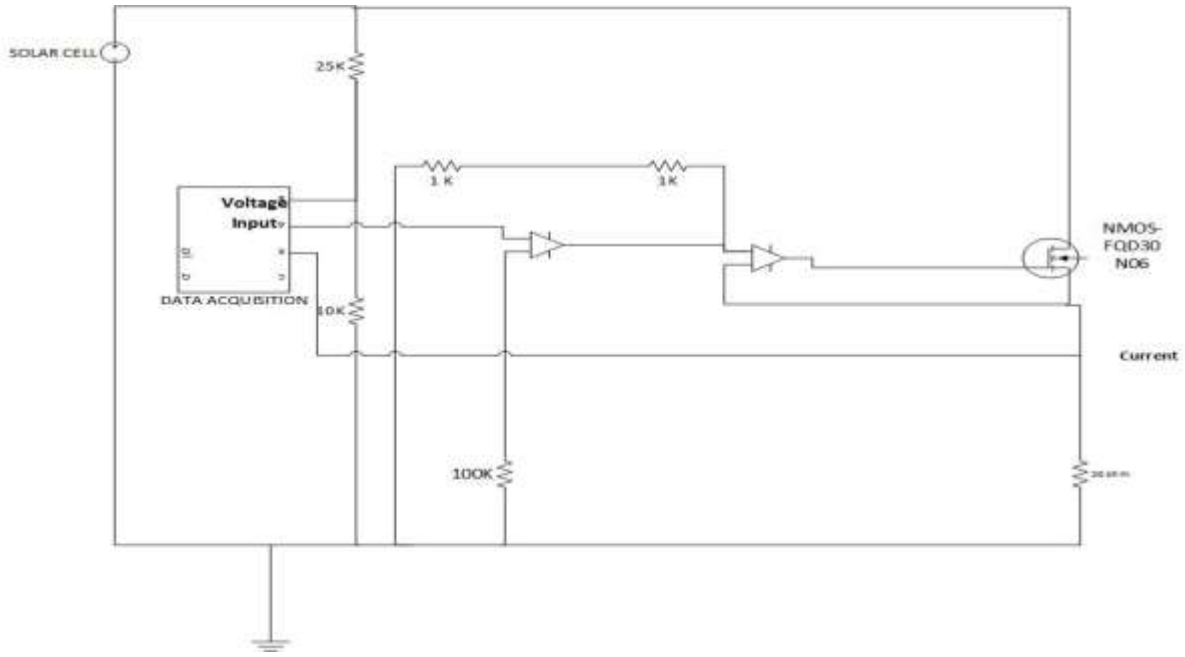

Figure 18: Designed circuit and data acquisition layout for curve tracing of PV cell

The data is acquired through an Arduino and the voltage across the gate is varied by using Pulse width modulation. The input is increased from 0-255 (0 to 5 Volts) through increments of +5(0.019V). The voltage is measured across drain terminal while the current is measured across the source terminal through a current sense resistor. The code for the Arduino is developed making the use of PWM and averaging functions.

c) Pseudo Code[3]:

The pseudo code for the program is as follows:

- Start:
- Include MAX6675 library for thermocouple,
- Initialize pins for max6675 variables SO, CS and CLK.
- Initialize variables for time and Arduino pins
- Declare variables for voltage and current,

[3] See APPENDIX B: ARDUINO CODE for original working code

- Declare variables for averaging functions and PWM.
- For readings 0 to 10

  Take values for voltage from Arduino,

  Add value to the voltage total

  Take values for current from Arduino,

  Add value to the current total
- Divide total by 10 for average values of voltage and current.
- Increase the value to the pin for PWM by 5 for increasing gate voltage
- Take value of temperature and store it in array of 55 elements for one cycle.
- If cycle is complete

  Display average temperature

  Reset temperature array element to 0

  Reset PWM value to 0
- Display the values of current, voltage, time and temperature at end of each iteration.
- Update the time by 0.5 seconds
- Give a delay of 500ms.

3.3.3.2 Flux measurement system (FSM)

A simple setup was designed and with this set calorimetric experiments were performed to calculate the flux output and its distribution. A 4cm by 4 cm aluminum 1100 square shaped with thickness of 3mm was placed with thermocouple and placed at targeted area. The plate reached to steady state temperature after few minutes. This indicate the average flux falling on the plate

a) Approach

Assuming steady state temperature, a simple energy balance cab be used to find out the flux output in terms of surface temperature and surface properties .Energy balance diagram is shown in Figure 19. The sides and bottom side was insulated with glass wool. The plate was modelled as horizontal plate with free convection and radiation heat transfer on top surface. The bottom and sides were considered insulated

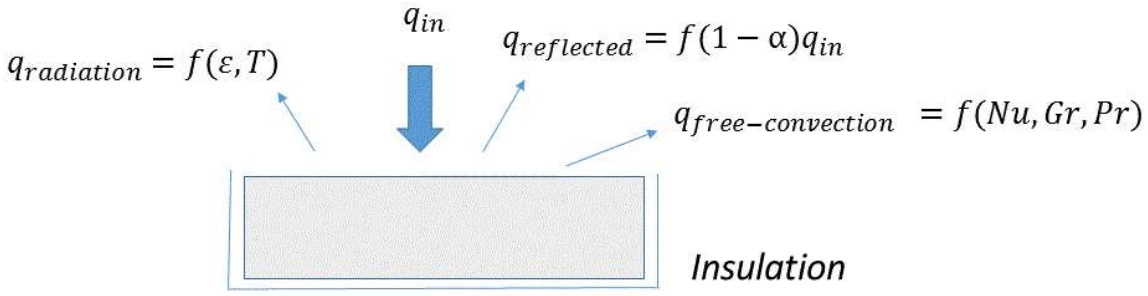

Figure 19:Enegry balance diagram of aluminum plate for flux measurent

$$q_{in} = q_{radiation} + q_{free\ convection} + q_{reflected} \tag{3.3}$$

Using standard relations from texts books of heat and mass transfer book[38]. Radiative heat flux loses, reflected loses and convective loses are calculated as follows:

$$q_{radiation=}\epsilon\sigma(T^4 - T_\infty^4) \tag{3.4}$$

$$q_{reflected} = (1-\alpha)q_{in} \tag{3.5}$$

$$q_{free\ convetion=}\ h(T - T_\infty) \tag{3.6}$$

where

$$h = Nu.k/L_c \tag{3.7}$$

$$Nu = 0.54Ra_{Lc}^{(1/4)} \tag{3.8}$$

$$Ra_{Lc=}\ \ (Pr)g\beta(T - T_\infty)/v^2 \tag{3.9}$$

$\boldsymbol{\sigma}$= Stefan-Boltzmann constant=5.67 x 10^{-8} W/$m^2.K^4$

$\boldsymbol{\varepsilon}$=Emissivity of Aluminum 1100

α= absorptivity of aluminum 1100

T= Surface temperature of plate of FSM measured by thermocouple, °C

T_∞=temperature of the fluid sufficiently far from the surface, °C

Pr = Prandtl number,

Ra_{Lc}=Rayleigh number

ν= kinematic viscosity of air , m^2/s

k= conductivity of air,$W/m^2.K$

L_c= Critical length, it is equal to one fourth of side of square

b) Final designed setup

Figure 20 shows the fabricated setup to measure the flux output .Aluminum plate is held in position with special designed fixture .Thermocouple is placed at back of plate. Back side is insulated with glass wool

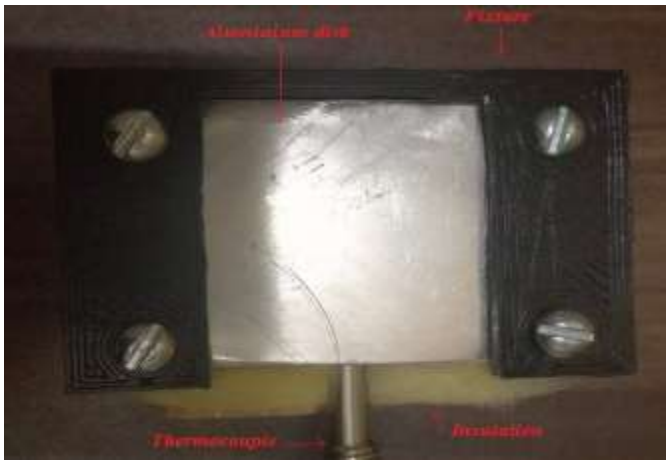

Figure 20: Flux measurment system (FSM)

3.3.3.3 Light spectrometer

For validation purposes, a spectrometer was needed which would be able to measure the wavelength of light so that a comparison can be made based on light spectrum of the sun and solar simulator. Different spectrometers were reviewed and the final decision was made based on accuracy and market availability. The mini USB spectrometer of Thunder Optics [39] can measure a light spectrum between the visible range(400-700 nm) of light.

Since Photovoltaic cells work only within the visible spectrum, so for our current purpose this spectrometer has proved to be quite useful, see Figure 21.

3.3.4 Metallic frame and other accessories

To hold all components together and in correct position a metallic frame was designed and manufactured .Other accessories includes wooden walls and glass wool for insulation. Blowers and exhaust fan were installed for cooling of fans .Power supply was also incorporated for lamp.

3.4 Complete solar simulator assembly

After all components designed and manufactured, they were assembled as shown in following Figure 22. All accessories were also incorporated in the assembled designed Accessories include cooling blowers, exhaust fan, wooden walls all around the metallic frame and glass wool to protect data acquisition devices from overheating. Solar simulator after fabrication is shown below in Figure 23 .

Figure 21.Mini USB spectrometer

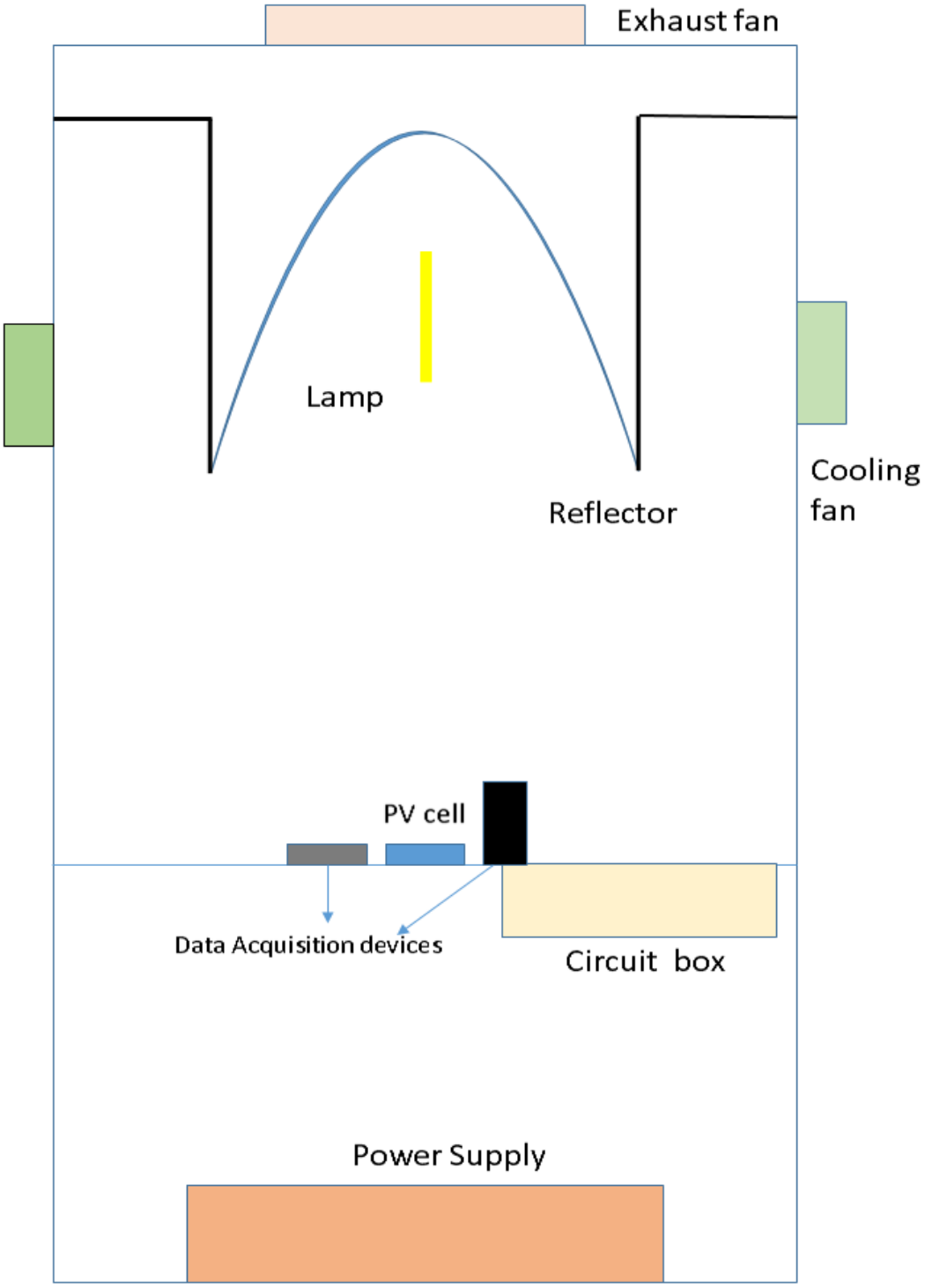

Figure 22 Schematic diagram of assembly of solar simulator components

Figure 23: Fabricted solar simulator

CHAPTER 4

RESULTS

This chapter describes the results of working of solar simulator after fabrication. Results includes the spectrum of light, its comparison to spectrum of sunlight and intensity distribution of solar simulator for evaluating how best the solar simulator is working to provide necessary and suitable conditions for PV cell testing. Plots of I-V curves and power-voltage curves of PV cell under sun light and under simulator light are also presented. In each heading there are two parts .Part (a) explains the results and part (b) explains conclusion drawn from these results.

Following details have been narrated in this chapter:

4.1 Spectrum of simulator light and its comparison with sun light

4.2 Flux output at targeted area of PV cell

4.3 PV cell curve tracing

4.4 Conclusion

4.1 Spectrum of simulator light and its comparison with sun light

Results:

a) Spectrum of sunlight was measured at different days and at different times. Sun spectrum remained constant thought these days as assumed. See Figure 24.

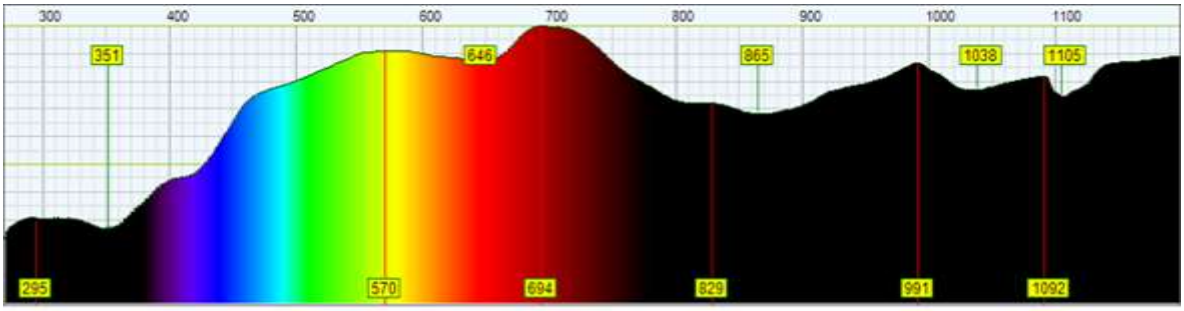

Sun spectrum at 12p.m on 18th May

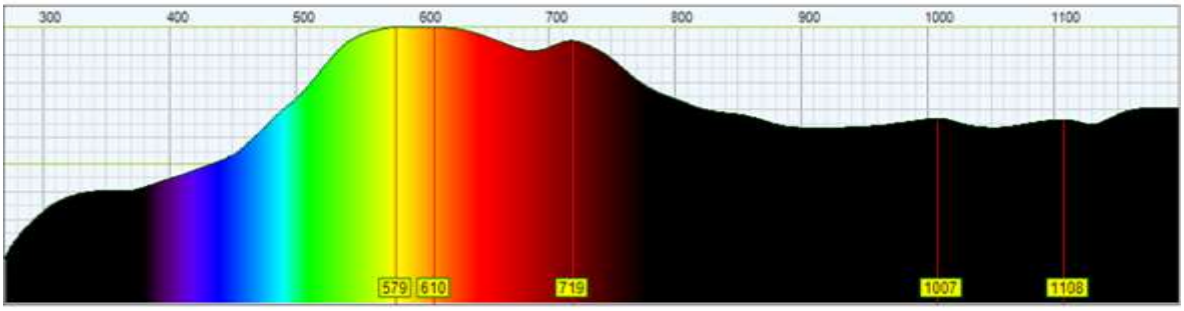

Sun spectrum at 3 p.m on 23rd May

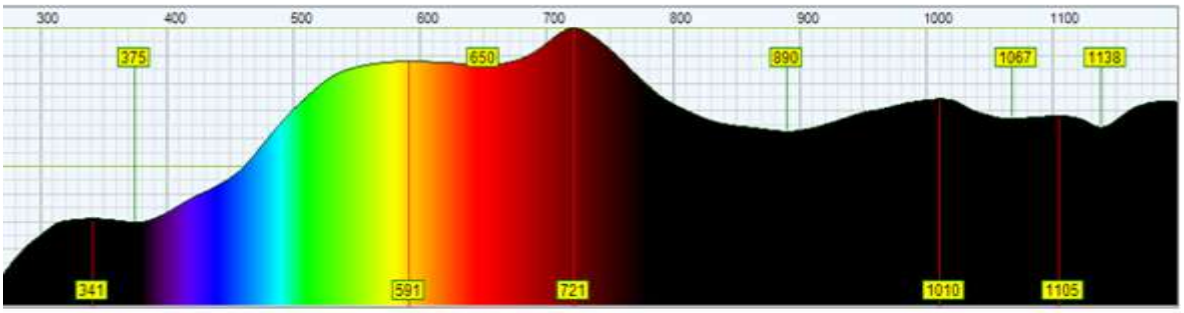

Sun spectrum at 12 p.m on 24th May

Figure 24: Spectrum of sun light

b) Now we compare the spectrum of simulator light to spectrum of sun light. See Figure 25:

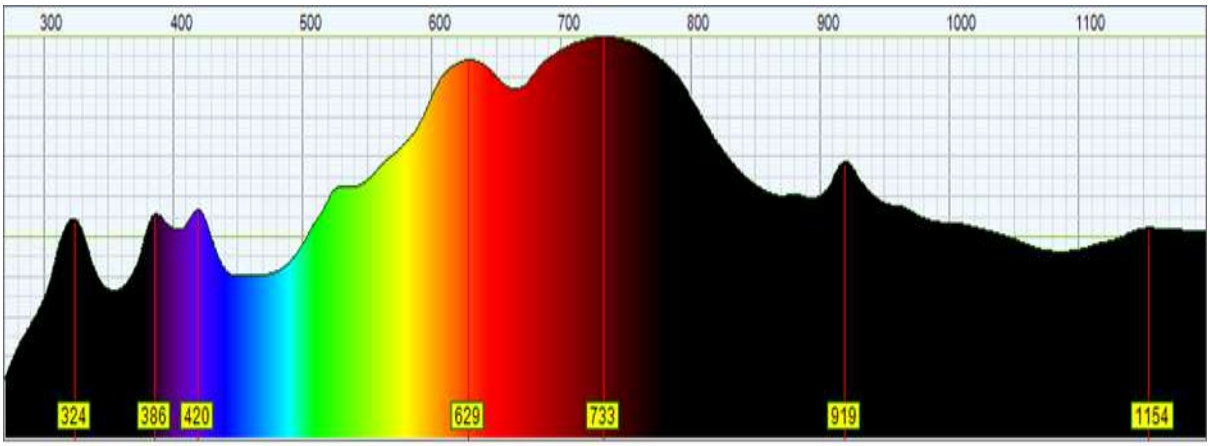

Spectrum of light of solar simultor

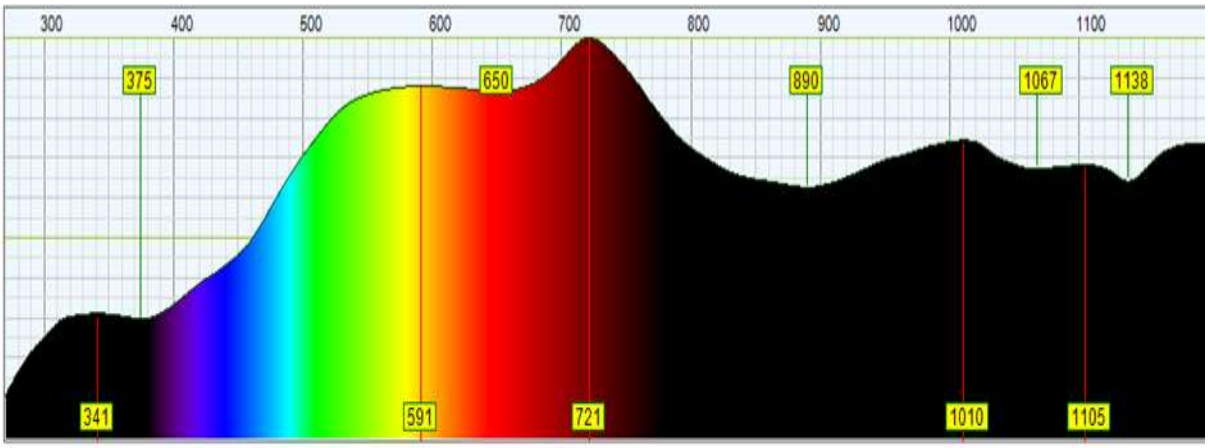

Spectrum of sun light at 1200 p.m 24th May

Figure 25: Comparison between spectrum of simulator light and spectrum sunlight

Assessment: In spectrum vertical axis shows the percentage of specific wavelength present in the total spectrum and horizontal axis shows the starting and ending point of specific color region .In terms of wavelengths present in spectrometer, both spectrum have same wavelengths with same starting and end points. However for percentages there are few differences. Differences are

1) Spectrum of light has more spikes than spectrum of sun. Spectrum of sun has smooth pattern

2) Indigo and dark blue region of light has relatively higher percentage as compared to same regions in sun spectrum

3) Light blue, green, and yellow regions of light has relatively lower percentages as compared to sum spectrum

4) Red colour region has almost same percentage in both spectrums

The above confirm that that the light spectrum of the solar simulator and sun are similar to a high degree. Most of spectrum of light is replica of solar spectrum. Thus one of the objectives of solar simulator has been achieved.

4.2 Flux output at targeted area of PV cell

Using designed flux measurement system and following properties of aluminum 1100[40-42] calorimetric experiments were carried out.

Emissivity	0.05
Reflection coefficient	0.86

Results: In 12-15 minutes, the aluminum plate got steady average temperature of 106°C in each experiment as shown in Figure 26.Thus using the approach mentioned earlier in section 3.3.3.2 Flux measurement system (FSM) and the average flux falling onto the plate found to be 1800W/m^2

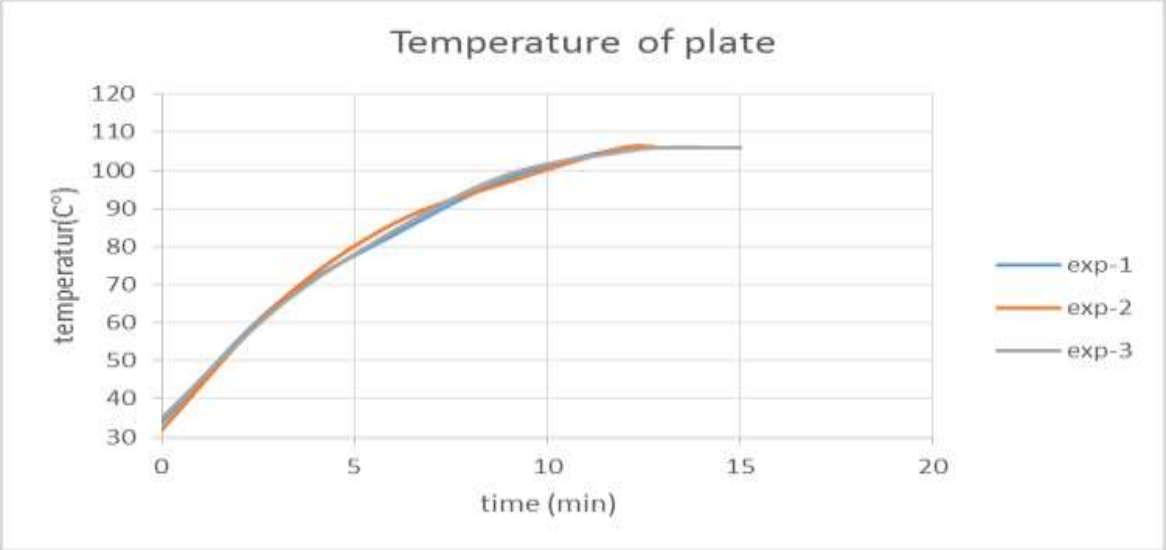

Figure 26 Temperature of aluminum plate of FSM with time

Assessment: Results have shown that average flux of 1800W/m^2 has been fallen onto the targeted area thus it is far more than the required value of 1000W/m^2. The temperature of 106°C has also been achieved for plate. This shows the over designing of solar simulator but it is good. Flux can be minimized by using filters for testing of PV cells. On the other hand, now we can use solar simulator for other tests due to its high flux .Test on materials and salts subjected to high temperature can be performed. Thus in this way, this designed solar simulator is proved to be multi-functional.

4.3 PV cell curve tracing

Results: The PV cell produces max current and voltage of about 200mA and 4V respectively. Under the light of the solar simulator we get current of about 250mA and voltage of 4.5 V. With increase in resistance across the cell the voltage increases while the current decreases. An increase in temperature of the cell results in decrease in the maximum voltage. When the light intensity is increased, the maximum current increases. These values of voltage and current for PV cell are used to make plots for the cell.

The results for an I-V curve from ambient room are depicted in the graph as in Figure 27.

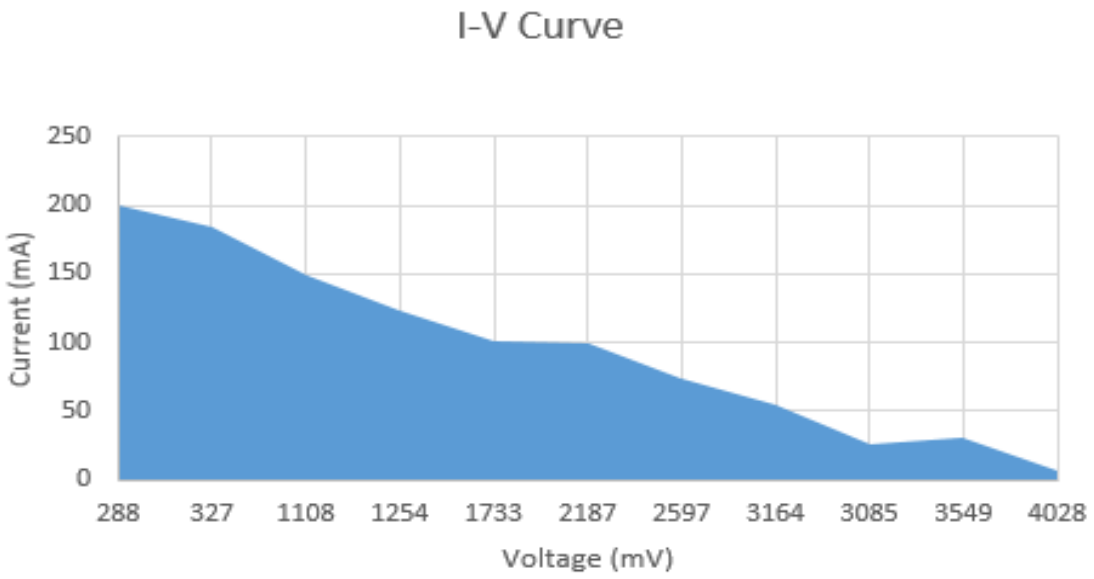

Figure 27: I-V curve for single PV cell under ambient light

The results from a test under the solar simulator show the following result shown in Figure 28

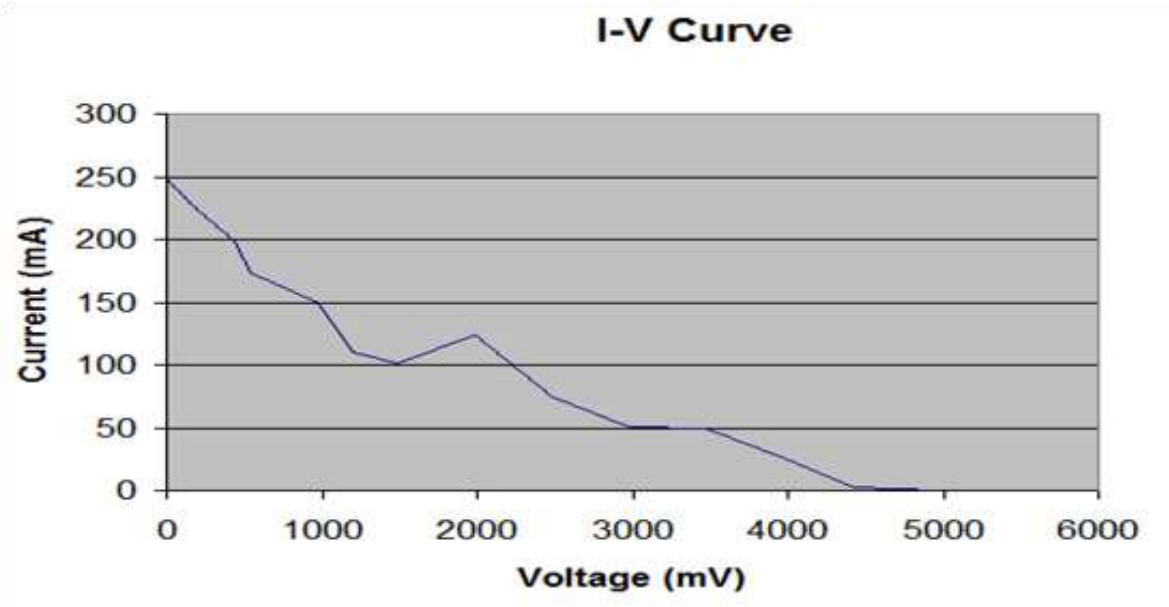

Figure 28: I-V curve of single silicon PV cell under simulator

Assessment: I-V curve tracer of solar simulator is good enough to plot such good curves. These curves are similar to general I-V curves of PV cell thus indicating that PV cell curve tracer is working in right manner. Thus PV cell curve tracer can be used to check performance of PV cell under light and in this way third objective of the project has been achieved

4.4 Conclusion

To conclude the chapter, all three primary objectives of solar simulator has been achieved.

1) Spectrum of light is close enough to spectrum of light in terms of colors and percentage of these colors in the spectrum

2) Output flux of light is more than 1000W/m^2 and thus required solar flux has been achieved

3) PV curve tracing system is working good enough to trace the I-V curves of cell, thus thermal characterization of cells can be made through this solar simulator

CHAPTER 5

CONCLUSION AND RECOMMENDATION

5.1 Conclusion

Solar simulator with its desired characteristics have been designed and fabricated successfully .It is totally functional and in working position .Contrary to commercial simulators, it has been equipped just with single metal halide lamp and single ellipsoidal reflector and capable enough to produce necessary conditions for said testing of photo voltaic (PV) cells.

It has following characteristics:

- Spectrum of simulator is fairly close enough in terms of wavelength present in it and energy distribution within these wavelengths to spectrum of sun light
- It is capable to give flux of minimum value of 1000 and maximum of
- PV cell curve tracing system makes it possible to plot performance curves of PV cell. Curves include I-V and power-voltage curves at different temperature of PV cell. In this way changes in efficiency and power output of PV cell can be observed and noted effectively.

5.2 Recommendations

1. For making comparison between different cooling techniques for performance enhancement of PV cells.

Other than thermal characterization of PV cells, this solar simulator can also be used to carry out study of different cooling techniques to enhance the efficiency and power output of PV cell. Although number of different studies has been done in this field, but in each different study, one or two cooling techniques have been studied .Thus due to different methodology of each study with different testing conditions, it seems impossible to make out comparison between different techniques and investigate which method is more effective .As we gone through literature related to studies of cooling techniques, it has been that each work reported different results with different testing conditions. Thus it was difficult to investigate that which method is more effective. Contrary, we tried to make

comparison. Three parameter were PV cell maximum temperature before cooling, minimum temperature after cooling and percentage increase in the efficiency. In this a rough comparison was as made as a shown in 3D below in Figure 29 .But this comparison could not suggest and give insight about a cooling method because there were lot of parameters missing. Thus we suggest that this simulator can be used for this comparison because one can perform all different techniques under same testing conditions and can report required performance parameters

Table 2: Key for 3D graph of different cooling methods for PV cell

Parameter of graph	**Meaning**
Outer radius of chunk	Temperature before cooling
Inner radius of chunk	Temperature after cooling
Height	Percentage increase in electrical efficiency

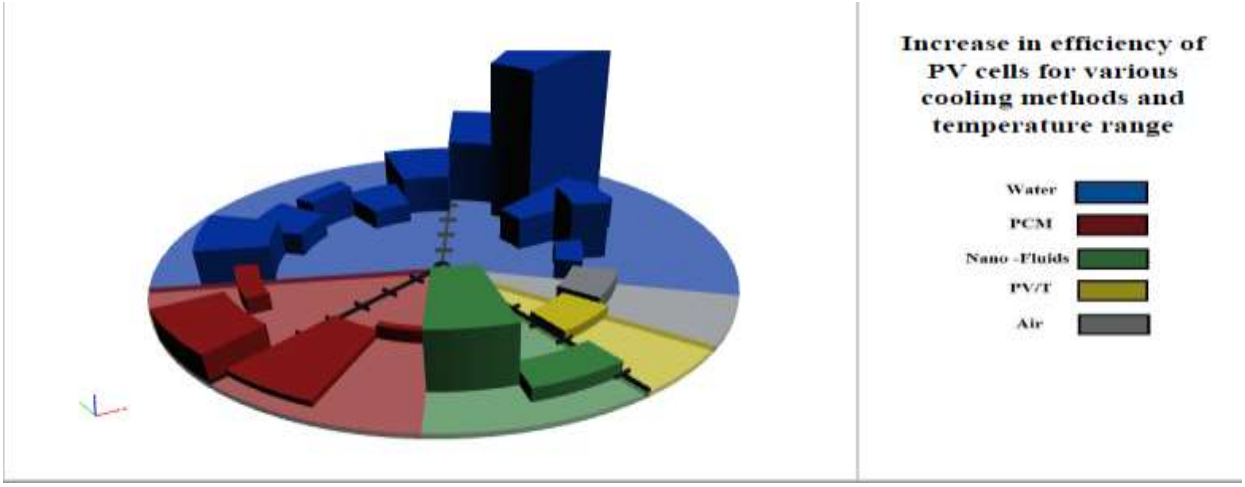

Figure 29: 3D graph for different cooling methods for PV cell

2) High flux studies

Due to high temperature and high flux of 1800W/m^2 at targeted area, this simulator can also be sued for high flux studies .It may include optical behavior and melting of salts, chemical reactions, thermal degradation of advanced materials, and biological studies such killing of cancerous cells.

WORKS CITED

1. Hasan, M.A. and K. Sumathy, *Photovoltaic thermal module concepts and their performance analysis: A review.* Renewable and Sustainable Energy Reviews, 2010. **14**(7): p. 1845-1859.
2. Tyagi, V.V., et al., *Progress in solar PV technology: Research and achievement.* Renewable and Sustainable Energy Reviews, 2013. **20**: p. 443-461.
3. Khan, H.A. and S. Pervaiz, *Technological review on solar PV in Pakistan: Scope, practices and recommendations for optimized system design.* Renewable and Sustainable Energy Reviews, 2013. **23**: p. 147-154.
4. Moharram, K.A., et al., *Enhancing the performance of photovoltaic panels by water cooling.* Ain Shams Engineering Journal, 2013. **4**(4): p. 869-877.
5. El Chaar, L., L.A. lamont, and N. El Zein, *Review of photovoltaic technologies.* Renewable and Sustainable Energy Reviews, 2011. **15**(5): p. 2165-2175.
6. Weakliem, H.A. and D. Redfield, *Temperature dependence of the optical properties of silicon.* Journal of Applied Physics, 1979. **50**(3): p. 1491.
7. Radziemska, E., *The effect of temperature on the power drop in crystalline silicon solar cells.* Renewable Energy, 2003. **28**(1): p. 1-12.
8. Cuce, E. and P.M. Cuce, *Improving thermodynamic performance parameters of silicon photovoltaic cells via air cooling.* International Journal of Ambient Energy, 2013. **35**(4): p. 193-199.
9. Krauter, S., *Increased electrical yield via water flow over the front of photovoltaic panels.* Solar Energy Materials and Solar Cells, 2004. **82**(1-2): p. 131-137.
10. Makki, A., S. Omer, and H. Sabir, *Advancements in hybrid photovoltaic systems for enhanced solar cells performance.* Renewable and Sustainable Energy Reviews, 2015. **41**: p. 658-684.
11. van Helden, W.G.J., R.J.C. van Zolingen, and H.A. Zondag, *PV thermal systems: PV panels supplying renewable electricity and heat.* Progress in Photovoltaics: Research and Applications, 2004. **12**(6): p. 415-426.
12. Baloch, A.A.B., et al., *Experimental and numerical performance analysis of a converging channel heat exchanger for PV cooling.* Energy Conversion and Management, 2015. **103**: p. 14-27.
13. Chandrasekar, M., et al., *Passive cooling of standalone flat PV module with cotton wick structures.* Energy Conversion and Management, 2013. **71**: p. 43-50.

14. Bahaidarah, H.M.S., *Experimental performance evaluation and modeling of jet impingement cooling for thermal management of photovoltaics.* Solar Energy, 2016. **135**: p. 605-617.

15. Stropnik, R. and U. Stritih, *Increasing the efficiency of PV panel with the use of PCM.* Renewable Energy, 2016. **97**: p. 671-679.

16. Sardarabadi, M. and M. Passandideh-Fard, *Experimental and numerical study of metal-oxides/water nanofluids as coolant in photovoltaic thermal systems (PVT).* Solar Energy Materials and Solar Cells, 2016. **157**: p. 533-542.

17. Karami, N. and M. Rahimi, *Heat transfer enhancement in a hybrid microchannel-photovoltaic cell using Boehmite nanofluid.* International Communications in Heat and Mass Transfer, 2014. **55**: p. 45-52.

18. Malik, A.Q. and S.J.B.H. Damit, *Outdoor testing of single crystal silicon solar cells.* Renewable Energy, 2003. **28**(9): p. 1433-1445.

19. Bahaidarah, H., et al., *Performance evaluation of a PV (photovoltaic) module by back surface water cooling for hot climatic conditions.* Energy, 2013. **59**: p. 445-453.

20. Maiti, S., K. Vyas, and P.K. Ghosh, *Performance of a silicon photovoltaic module under enhanced illumination and selective filtration of incoming radiation with simultaneous cooling.* Solar Energy, 2010. **84**(8): p. 1439-1444.

21. Kuhn, P. and A. Hunt, *A new solar simulator to study high temperature solid-state reactions with highly concentrated radiation.* Solar Energy Materials, 1991. **24**(1): p. 742-750.

22. Petrasch, J., et al., *A Novel 50 kW11,000 suns High-Flux Solar Simulator Based on an Array of Xenon Arc Lamps* Solar Energy, 2007.

23. Codd, D.S., et al., *A low cost high flux solar simulator.* Solar Energy, 2010. **84**(12): p. 2202-2212.

24. Sarwar, J., et al., *Description and characterization of an adjustable flux solar simulator for solar thermal, thermochemical and photovoltaic applications.* Solar Energy, 2014. **100**: p. 179-194.

25. Ekman, B.M., G. Brooks, and M. Akbar Rhamdhani, *Development of high flux solar simulators for solar thermal research.* Solar Energy Materials and Solar Cells, 2015. **141**: p. 436-446.

26. Okuhara, Y., et al., *A Solar Simulator for the Measurement of Heat Collection Efficiency of Parabolic Trough Receivers.* Energy Procedia, 2015. **69**: p. 1911-1920.

27. Meng, Q., Y. Wang, and L. Zhang, *Irradiance characteristics and optimization design of a large-scale solar simulator.* Solar Energy, 2011. **85**(9): p. 1758-1767.

28. Wang, W., et al., *Design and Validation of a Low-cost High-flux Solar Simulator using Fresnel Lens Concentrators.* Energy Procedia, 2014. **49**: p. 2221-2230.

29. Mantosh K. Chawla Photo Emission Tech., I. *A step by step guide to selecting the "right" Solar Simulator for your solar cell testing application*.

30. Atkin, P. and M.M. Farid, *Improving the efficiency of photovoltaic cells using PCM infused graphite and aluminium fins.* Solar Energy, 2015. **114**: p. 217-228.

31. Maiti, S., et al., *Self regulation of photovoltaic module temperature in V-trough using a metal–wax composite phase change matrix.* Solar Energy, 2011. **85**(9): p. 1805-1816.

32. Ebrahimi, M., M. Rahimi, and A. Rahimi, *An experimental study on using natural vaporization for cooling of a photovoltaic solar cell.* International Communications in Heat and Mass Transfer, 2015. **65**: p. 22-30.

33. Al-Shohani, W.A.M., R. Al-Dadah, and S. Mahmoud, *Reducing the thermal load of a photovoltaic module through an optical water filter.* Applied Thermal Engineering, 2016. **109, Part A**: p. 475-486.

34. Santos-González, I., et al., *Numerical modeling and experimental analysis of the thermal performance of a Compound Parabolic Concentrator.* Applied Thermal Engineering, 2017. **114**: p. 1152-1160.

35. Ustaoglu, A., et al., *Evaluation of the efficiency of dual compound parabolic and involute concentrator.* Energy for Sustainable Development, 2016. **32**: p. 1-13.

36. Lin, S.H. and E.M. Sparrow, *Radiant Interchange Among Curved Specularly Reflecting Surfaces—Application to Cylindrical and Conical Cavities.* Journal of Heat Transfer, 1965. **87**(2): p. 299-307.

37. Steinfeld, A., *Exchange factor between two spheres placed at the foci of a specularly reflecting ellipsoidal cavity.* International Communications in Heat and Mass Transfer, 1991. **18**(1): p. 19-26.

38. *Çengel, Y.A., Heat and mass transfer : a practical approach2007, Boston [u.a.]: McGraw-Hill.*

39. *http://www.thunderoptics.fr/index.php?p=1_22_Mini-USB-SPectrometer.*

40. International, A., *Metals Handbook, Vol.2 - Properties and Selection: Nonferrous Alloys and Special-Purpose Materials, ASM International 10th Ed. 1990.*

41. International, A., *Metals Handbook, Howard E. Boyer and Timothy L. Gall, Eds., American Society for Metals, Materials Park, OH, 1985.*

42. INTERNATIONAL, A., *Structural Alloys Handbook, 1996 edition, John M. (Tim) Holt, Technical Ed; C. Y. Ho, Ed., CINDAS/Purdue University, West Lafayette, IN, 1996.*

APPENDIX A: DERIVATIONS OF ANALYTICAL RELATIONS FOR REFLECTOR

This appendix contains derivations of analytical relations for ellipsoidal reflector based on laws of reflection and trigonometry.

Ellipsoidal reflector is surface of revolution .It is formed by revolving a planar ellipse about its major axis. Ellipse has following geometrical parameters as shown in **Error! Reference ource not found.**.It has two focus points. Foci of ellipse lie on major axis (a). Major axis (2*a*) and focal length *(2c)* are related to each other through eccentricity *e* as *e=c/a* and minor axis *(2b*) is related to major axis as $b=\sqrt{(a^2 - c^2)}$.When point light source is placed at focus F1, then after single specular reflection it is converged to second focus F2 as shown in Figure 31.

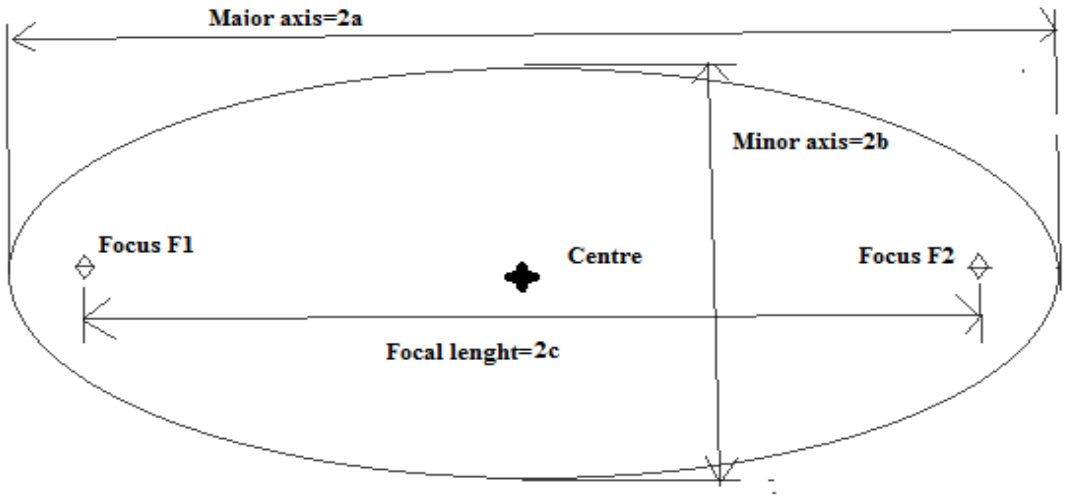

Figure 30: Planar Ellipse

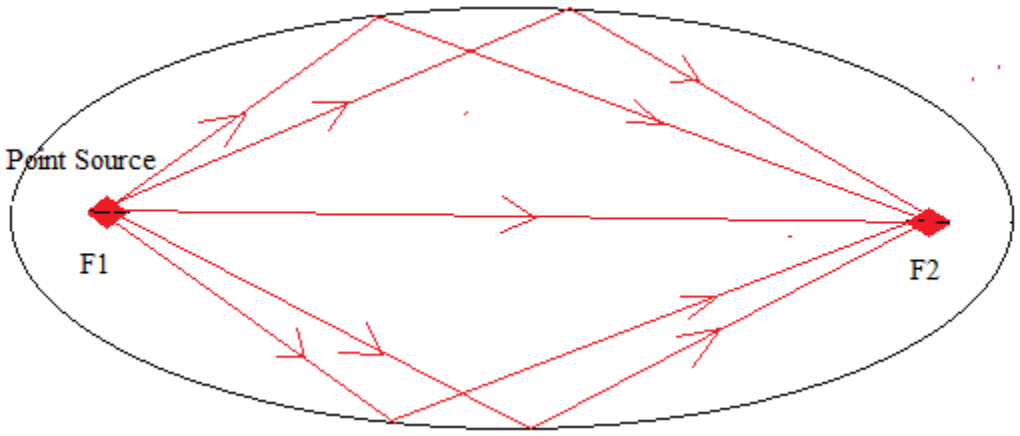

Figure 31: Planar ellipse with point light source

A) Magnified arc size *M1′* due to right end of reflector

Ellipsoidal reflector are normally used in truncated form. From Figure 32. of truncated reflector and using trigonometry

$$x(mm) = \frac{0.5d}{tan60°} \tag{A.1}$$

$$x(mm) = 0.28867d \tag{A.2}$$

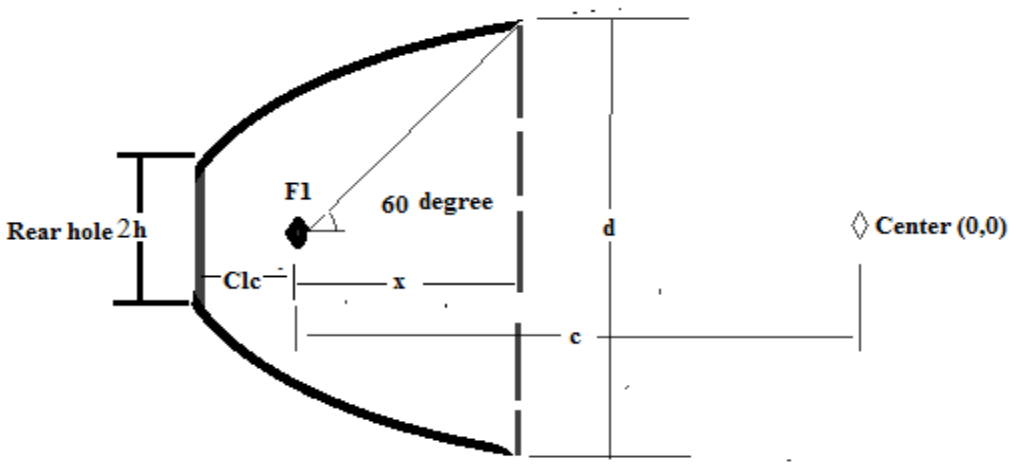

Figure 32 Reflectro truncated at 60°

The lamp will be placed along the major axis in such a way that arc midpoint points coincides with focus F1. The ray **(*a'*)** starting from right end B of arc will hit the reflector end at point C, by making **angle α** with vertical CD, and will be reflected in such way that it will reach point E in line with the second focus F2. The ray **(*b'*)** starting from right end A of arc will hit the reflector end at point C, by making **angle β** with vertical CD, and will be reflected in such way that it will reach point F in line with the second focus F2.The ray originating from focus F1, will reach second focus F2. In this arc is magnified. Assuming the arc is magnified by equally on both sides of focus F2.The half of magnification has been label ***M1***.

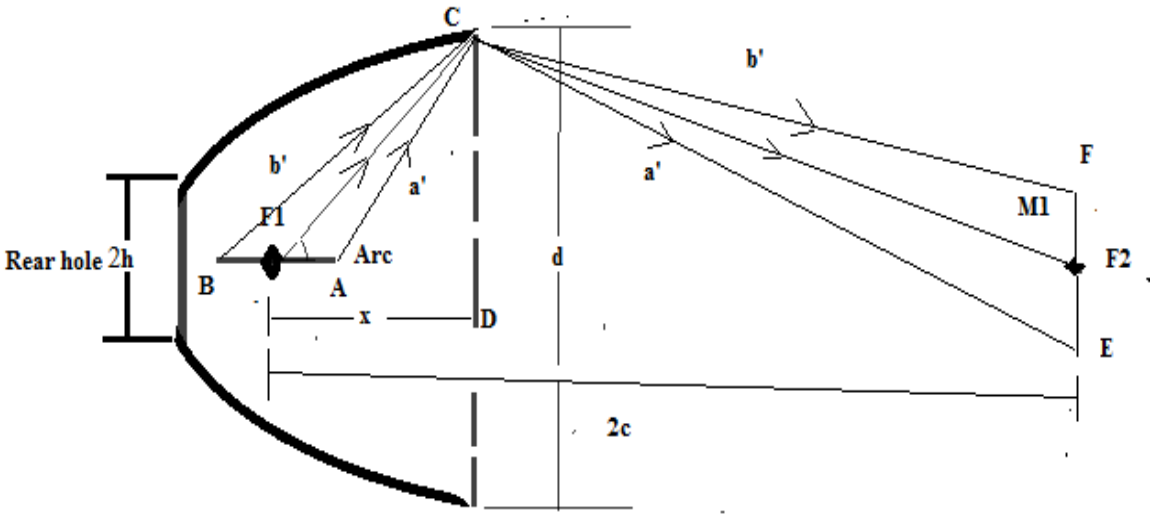

Figure 33: Half of arc magnified size , M1 due to right end of reflector

From trigonometry, right angled triangles *ACD* and *BCD* from Figure 33:

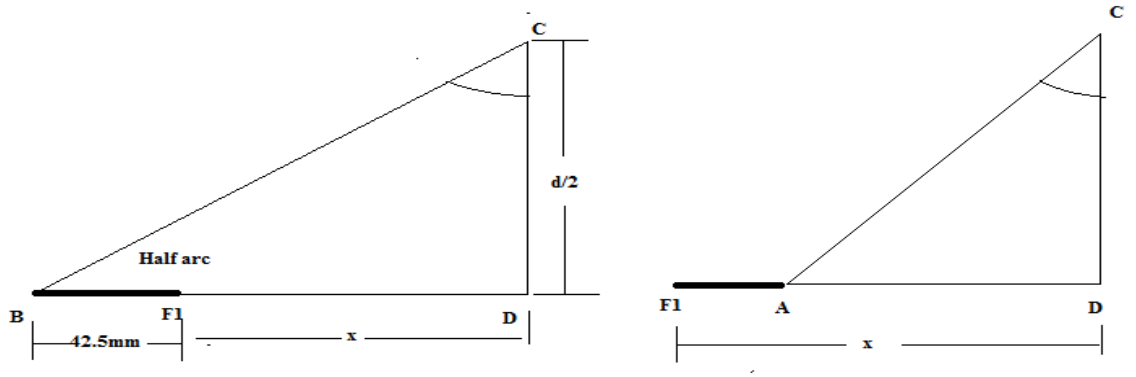

Figure 34: Right triangles ACD and BCD

$$\alpha(degree) = 57.295(tan^{-1}\ \frac{x - 42.5}{d/2}) \tag{A.3}$$

$$\beta(degree) = 57.295(tan^{-1}\ \frac{x + 42.5}{d/2}) \tag{A.4}$$

The mid ray from focus F1 divides the angle **α-β (α minus β)** and thus each ray either **(*a*´)** or **(*b*´)** makes half of angle with mid ray (verified by sketching in Solid Works) named as **γ** where

$$\gamma(degree) = \frac{(\alpha - \beta)}{2} \tag{A.5}$$

For calculating half of magnified size of arc **M1** after the reflection at second focus F2, consider right triangles *CFK* and *DF2C* from Figure 33.

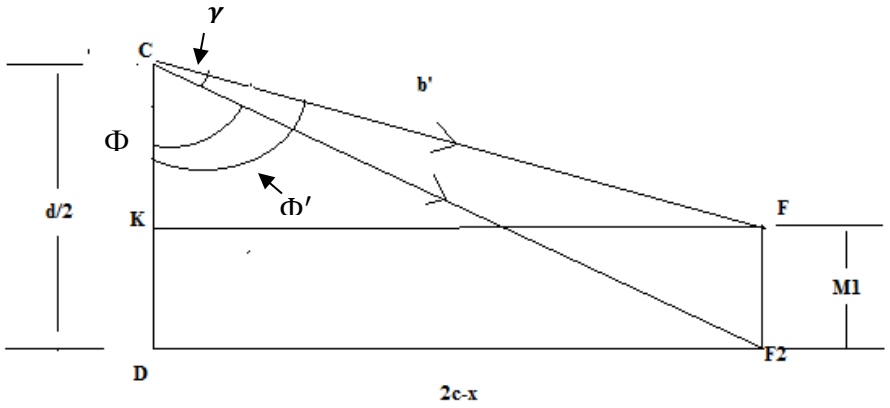

Figure 35: Right trinagles CFK and DF2C for M1

From triangle DF2C **angle** Φ' can be written as $\Phi' = \Phi + \boldsymbol{\gamma}$ because **ray** $\boldsymbol{b'}$ will make the same angle with the mid ray according to laws of reflection.Φ' can be written as

$$\Phi' \ (degree) = 57.295 \ tan^{-1}(4c - 0.5773) + \gamma \tag{A.6}$$

From triangle *CFK*

$$M1(mm) = (\frac{d}{2} - \frac{2c - 0.2886d}{tan\left(\frac{\Phi'}{57.295}\right)}) \tag{A.7}$$

And total magnified size M1′ is

$$M1'(mm) = 2M1 \tag{A.8}$$

B) Clearance between rear end and focus F1 (*Clc*)

Consider the following Figure 36. Line L is directrix of ellipse and it is always at distance of $\boldsymbol{c/e^2}$ from center (0, 0) of ellipse. The clearance between focus F1 and rear end is named as ***Clc***. Point P is at the rear end of reflector. The diameter of hole at rear end is 2***h.***

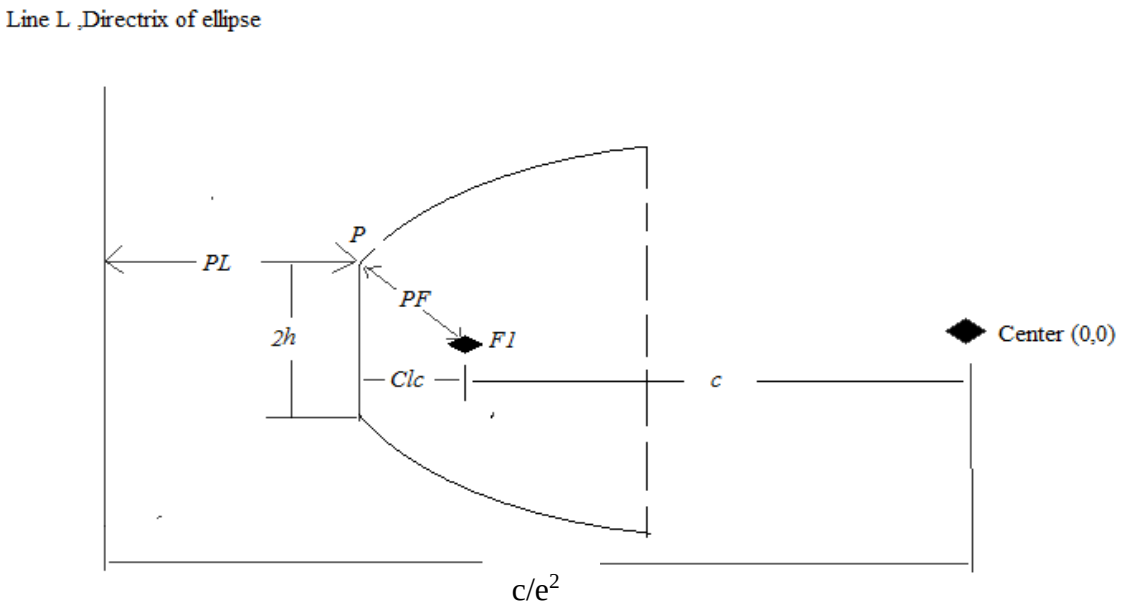

Figure 36: Ellipse with directrix

For ellipse the eccentricity (e) can be defined as

$$e = \frac{PF}{PL}$$

Where (from Fig.5)

$$PF = \sqrt{(Clc^2} + h^2)$$

$$PL = \frac{c}{e^2} - c - Clc$$

And

$$PF = (e)PL$$

$$PF = \left(\frac{c}{e} - ce\right) - Clc(e)$$

$$= (a - ce) - (e)Clc$$

$$Clc^2 + h^2 = ((a - ce) - (e)Clc)^2$$

$$= (a - ce)^2 - 2Clc(e) + \left((e)Clc\right)^2$$

Rearranging we get

$$Clc^2(1-e^2)+2Clc(e)(a-ce)+h^2-(a-ce)^2=0$$

Applying quadratic formula we have

$$\boldsymbol{Clc(mm)=\frac{-2e(a-ce)\pm\sqrt{4e^2(a-ce)^2+4(1-e^2)(h^2-(a-ce)^2)}}{2(1-e^2)}} \quad \text{(A.9)}$$

C) Magnified size *M2′* due to rear end of reflector

The **ray (*i′*)** starting from right end A of arc will hit the reflector rear end at point N, by making **angle ω** with vertical CD, and will be reflected in such way that it will reach point S in line with the second focus F2. The **ray (*j′*)** starting from left end B of arc will hit the reflector end at point N, by making **angle ψ** with vertical CD, and will be reflected in such way that it will reach point T in line with the second focus F2.The ray originating from focus F1, will reach second focus F2. In this arc is magnified. Assuming the arc is magnified by equally on both sides of focus F2.The half of this magnification has been labelled **M2** in Figure 37.

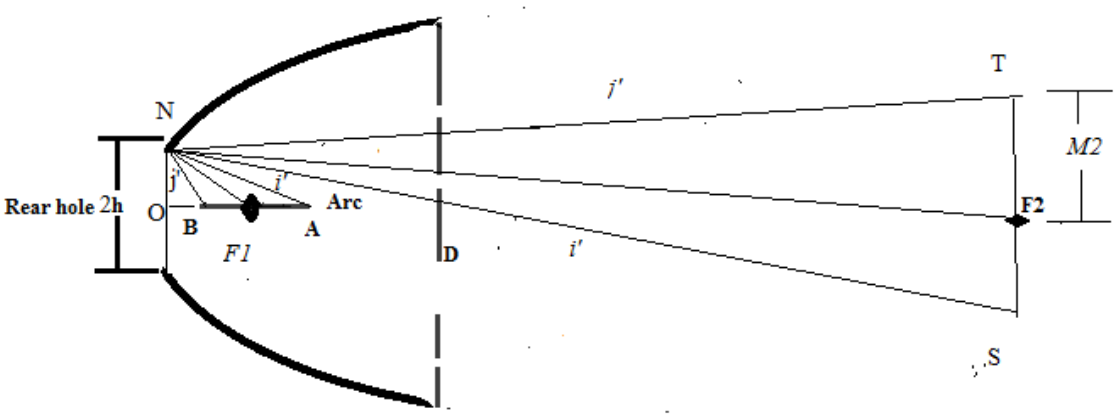

Figure 37: Half of arc magnified size , M2 due to rear end of reflector

Using same method as done for magnification *M1*, the angles *ω and ψ* can be written using triangles BON and AON from Figure 37 as

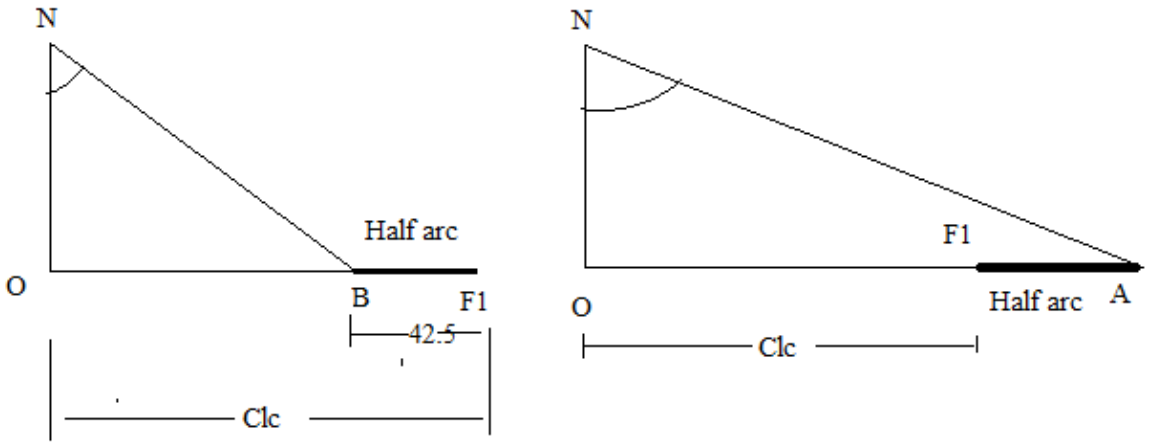

Figure 38 : Right triangles BON and AON for M2

$$\omega(degree) = 57.295 tan^{-1}\left(\frac{Clc + 42.5}{h}\right) \quad \text{(A.10)}$$

$$\psi(degree) = 57.295 tan^{-1}\left(\frac{Clc - 42.5}{h}\right) \quad \text{(A.11)}$$

The mid ray from focus F1 divides the **angle ω-ψ** and thus each ray **either (i′) or (j′**) makes half of angle (ω-ψ) with mid ray (verified by software analysis) named as **φ**

$$\varphi(degree) = \frac{(\omega - \psi)}{2} \quad \text{(A.12)}$$

For calculating magnification *M2* after the reflection at second focus F2, consider right triangles *NTQ* and *NF2Q*.

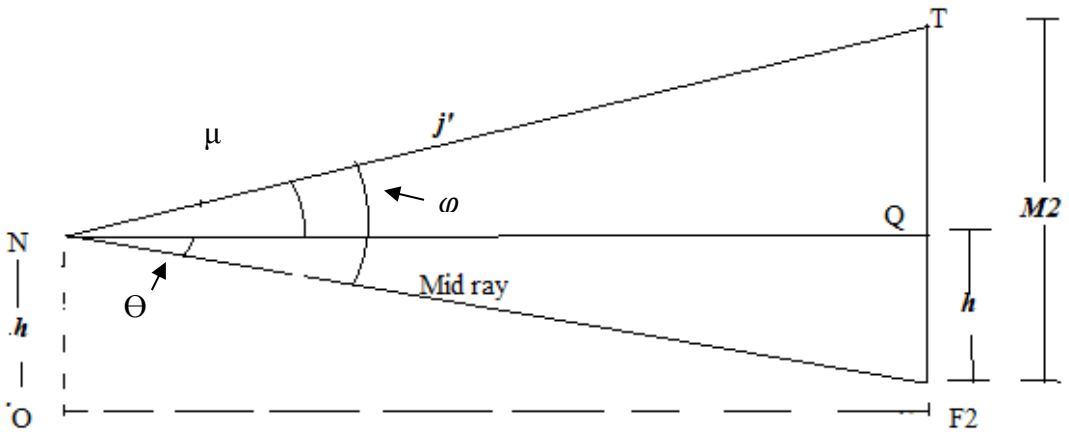

Figure 39 Right triangles NTQ and NF2Q for M2

From laws of reflection **ray (*j'*)** after reflection will make same angle φ with the mid ray. This angle is sum of **angle Θ** and **angle μ,** where

$$\theta = 57.295 tan^{-1}\left(\frac{h}{(2c + Clc)}\right) \quad \text{(A.13)}$$

$$\mu(\text{degree}) = \varphi - \theta \quad \text{(A.14)}$$

$$M2(mm) = h + \tan(\mu)\,(2c + Clc) \quad \text{(A.15)}$$

And total magnified size M2′ is

$$M2'(mm) = 2M2 \quad \text{(A.16)}$$

APPENDIX B: ARDUINO CODE

This appendix contains the Arduino code for acquiring data form PV cell.

```
#include "max6675.h"
 //adds the MAX6675 library for using thermocouple with Arduino
int ktcSO = 8;
int ktcCS = 9;
int ktcCLK = 10;
//Thermocouple Pins
double Time=0; //duration of program
MAX6675 ktc(ktcCLK, ktcCS, ktcSO);
const int ar= 55;//constant for finding average temperature over 55 steps
int value=0; // for  taking values for avg temperature
const int analogIn = A0;
const int analogIn1 = A1;
int Volt=0;
double Volta = 0;
double Amps = 0;
double x[ar];
const int NumReads=10 ;//for averaging current and voltage
double Total=0;
double Avg=0;
double Total1=0;
```

```
double Avg1=0;
double Total2=0;
double Avg2=0;
double Var=0; //variable for PWM
double cha=5; //increment for PWM
int led=6;// pin for PWM
double R=20; // resistance of current sense resistor
void setup(){
 Serial.begin(9600);
 delay(500);
}
void loop(){
  for(int ThisRead =0; ThisRead < NumReads ; ThisRead++)
 {
  Total=Total + analogRead(analogIn);
 Total1=Total1 + analogRead(analogIn1);
 }
analogWrite(led,Var); // for input to the NMOS gate
  Var= Var + cha;
  if (Var >=255)
  {
    Serial.print("\t \t Avg Temperature = ");
 Serial.print(Avg2,3);
```

```
//Prints average temperature at end of each cycle
   Var=0;
   Total2=Avg2;
   }
 Avg= Total/NumReads;
 Avg1= Total1/NumReads;
 Volt =Avg;
 Volta=Avg1;
 Volt = (Volt / 1024.0) * 5000; // Gets you mV
Volta = (Volta / 1024.0) * 500;
Amps= Volta/R;
Serial.print("\t \t input Value = " ); // shows input value
 Serial.print(Var);
Serial.print("\t \t Voltage (mV) = "); // shows the voltage measured
Serial.print(Voltage,3);
Serial.print("\t \t Current(mA) = ");//shows the measured current
 Serial.print(Amps,3);
 x[value]=ktc.readCelsius();
 Total2=Total2 + x[value];//measures average temperature
 Avg2 =Total2/ar;
          value=value+1;
          If (value>55)
{
```

```
value=0;
}
Total=0;
 Total1=0;
Serial.print(" \t Time = ");
 Serial.print(Time);
 Serial.print("\t Deg C = ");
 Serial.print(ktc.readCelsius());
 Serial.print("\t Deg F = ");
 Serial.println(ktc.readFahrenheit());
 Time=  Time + 0.5;//increase time by 0.5 seconds
   delay(500);//gives a delay of 500 ms
 }
```